dEHBP1 controls exocytosis and recycling of Delta during asymmetric divisions

Nikolaos Giagtzoglou,[1] Shinya Yamamoto,[2] Diana Zitserman,[5] Hillary K. Graves,[2] Karen L. Schulze,[1] Hao Wang,[3] Hayley Klein,[3] Fabrice Roegiers,[5] and Hugo J. Bellen[1,2,3,4]

[1]Howard Hughes Medical Institute, [2]Program in Developmental Biology, [3]Department of Molecular and Human Genetics, and [4]Department of Neuroscience, Baylor College of Medicine, Houston, TX 77030
[5]Fox Chase Cancer Center, Philadelphia, PA 19111

Notch signaling governs binary cell fate determination in asymmetrically dividing cells. Through a forward genetic screen we identified the fly homologue of Eps15 homology domain containing protein-binding protein 1 (dEHBP1) as a novel regulator of Notch signaling in asymmetrically dividing cells. dEHBP1 is enriched basally and at the actin-rich interface of pII cells of the external mechanosensory organs, where Notch signaling occurs. Loss of function of dEHBP1 leads to up-regulation of Sanpodo, a regulator of Notch signaling, and aberrant trafficking of the Notch ligand, Delta. Furthermore, Sec15 and Rab11, which have been previously shown to regulate the localization of Delta, physically interact with dEHBP1. We propose that dEHBP1 functions as an adaptor molecule for the exocytosis and recycling of Delta, thereby affecting cell fate decisions in asymmetrically dividing cells.

Introduction

Notch signaling is an evolutionarily conserved, intercellular signaling pathway that plays a seminal role in numerous biological processes, including cell fate acquisition and differentiation (Artavanis-Tsakonas et al., 1999; Bray, 2006; Fortini, 2009; Fortini and Bilder, 2009; Kopan and Ilagan, 2009; Tien et al., 2009). The versatile role of Notch signaling during development and adult tissue homeostasis relies upon the context-dependent function of different regulators and downstream effectors (Bray, 2006; Yamamoto et al., 2010). Given the importance of Notch signaling in development, cancer, and human diseases (Gridley, 2003, 2007; Weng and Aster, 2004; Roy et al., 2007; Watt et al., 2008; Bolós et al., 2009), the identification of new regulators of Notch (Berdnik et al., 2002; Sasamura et al., 2003; Hutterer and Knoblich, 2005; Jafar-Nejad et al., 2005; Vaccari and Bilder, 2005; Gallagher and Knoblich, 2006; Acar et al., 2008; Tien et al., 2008; Rajan et al., 2009; Saj et al., 2010; Vaccari et al., 2010) has played an important role in advancing our understanding of the molecular and cellular basis of development and disease. To understand the mechanisms of activation and identify novel regulators of Notch signaling, we performed forward genetic screens to identify genes that affect the asymmetric divisions of cells of the external sensory organs (ESOs), in which cell fate decisions depend on Notch signaling (Lai, 2004; Le Borgne et al., 2005; Gönczy, 2008).

The ESO lineages give rise to micro- and macrochaetae, which develop on the thoraces and appendages of adult flies in a highly organized pattern (Gho et al., 1999; Reddy and Rodrigues, 1999; Bellaïche and Schweisguth, 2001; Lai, 2004; Lai and Orgogozo, 2004; Le Borgne et al., 2005). Each ESO consists of four cells that develop from a single precursor, hereafter named the pI cell, through consecutive rounds of asymmetric divisions (Fig. 1 a). In the microchaetae lineages, the pI cell divides into a posterior pIIa and an anterior pIIb cell. The pIIa cell gives rise to the trichogen (shaft) cell and its surrounding tormogen (socket) cell, both visible on the exterior surface of the thoracic cuticle. The pIIb cell divides into a pIIIb and a glial cell, which migrates away and eventually dies. The pIIIb cell produces the neuron and the thecogen (sheath) cells.

N. Giagtzoglou and S. Yamamoto contributed equally to this paper.

Correspondence to Hugo J. Bellen: hbellen@bcm.edu

H.K. Graves' present address is Department of Biochemistry and Molecular Biology, The University of Texas, M.D. Anderson Cancer Center, Houston, TX 77030.

Abbreviations used in this paper: APF, after puparium formation; Arm, Armadillo; ARS, actin-rich structure; dEHBP1, Eps15 homology domain containing protein-binding protein 1; EHD, Eps15 homology domain; ESO, external sensory organ; Neur, Neuralized; Sens, Sensless; Spdo, Sanpodo.

Supplemental material can be found at:
http://doi.org/10.1083/jcb.201106088

The Rockefeller University Press $30.00
J. Cell Biol. Vol. 196 No. 1 65–83
www.jcb.org/cgi/doi/10.1083/jcb.201106088

The efficacy and directionality of Notch signaling during asymmetric divisions is accomplished at multiple levels by asymmetric endocytosis (Fürthauer and González-Gaitán, 2009a,b). Endosomes that are positive for SMAD anchor for receptor activation (SARA) are segregated asymmetrically, but loss of function of SARA does not lead to cell fate transformation defects in the ESO lineage (Coumailleau et al., 2009). The cell fate determinants Numb and Neuralized (Neur) form a crescent at the anterior cell cortex of pI in a Par complex–dependent manner (Betschinger et al., 2003; Langevin et al., 2005; Roegiers et al., 2005; Wirtz-Peitz et al., 2008) and segregate into the anterior pIIb signal–sending cell, where they function as regulators of vesicular trafficking. In the pIIa signal–receiving cell, which does not inherit Numb, Sanpodo (Spdo) localizes at the plasma membrane together with the Notch receptor where it positively regulates Notch function (O'Connor-Giles and Skeath, 2003; Hutterer and Knoblich, 2005; Langevin et al., 2005). In the pIIb cell, Numb inhibits the plasma membrane localization of Spdo and converts Spdo into a negative regulator of Notch (Babaoglan et al., 2009). In addition to Numb, Neur, an E3 ubiquitin ligase, controls the ubiquitination and endocytosis of Delta (Lai and Rubin, 2001; Pavlopoulos et al., 2001) in the signal-sending pIIb cell (Le Borgne and Schweisguth, 2003).

Delta endocytosis in the pIIb signal–sending cell may serve the purpose of "pulling" the Notch receptor via their physical interaction away from the cell receiving the Notch signal, possibly rendering the target sites of various proteases in Notch accessible to proteolytic cleavages. These cleavages are necessary for Notch activation (Parks et al., 2000; Nichols et al., 2007a,b). A nonexclusive model is the "recycling" model (Fig. 1 b). In this model, Delta is first inserted into the plasma membrane, but it is unable to signal. Delta is then endocytosed in a vesicular compartment. These Delta-bearing vesicles return back to a specialized plasma membrane domain at the interface of pIIa and pIIb cells, where the actin-rich structure (ARS) resides (Rajan et al., 2009). This process is mediated via a Rab11-positive recycling endosomal compartment (Emery et al., 2005; Benhra et al., 2011). Furthermore, loss of Sec15, a member of the exocyst complex and an effector of Rab11, leads to a basal accumulation of Delta and Spdo (Jafar-Nejad et al., 2005).

In the present study, we report the identification of *CG15609*, the *Drosophila* homologue of Eps15 homology domain containing protein-binding protein 1 (dEHBP1), as a novel component of Notch signaling during asymmetric cell divisions of the ESO lineages. We show that dEHBP1 regulates the levels and localization of Spdo as well as the trafficking of Delta at the signaling interface of the pIIa/pIIb. These data provide critical links between the key players required for the trafficking of Delta.

Results

2R11 regulates Notch signaling during asymmetric divisions in the ESO lineage

To identify novel genes in the Notch signaling pathway we performed a forward genetic mosaic screen on chromosome arm 2R to isolate mutations that disrupt the stereotypic pattern of the mechanosensory bristles on the thorax of the adult flies (Andrews et al., 2009). Mutations in the *2R11* complementation group are homozygous lethal and clones of these mutations on the adult thorax bear no bristles (Fig. 1, c and d). The *2R11* group consists of four alleles: *A28*, *O4*, *N8*, and *T14*.

To assess if the lack of bristles in the *2R11* mutant clones is due to loss of sensory precursor pI cells, we stained pupal thoraces at 15 h after puparium formation (APF) with anti-Senseless (Sens) antibody, which marks the pI and its progeny pII cells (Nolo et al., 2000). The emergence of Sens-positive pI cells is not affected within mutant regions of pupal thoraces (unpublished data). To examine whether the cell fates in the ESO lineages are affected, we assessed the expression of appropriate cell fate markers at 24–26 h APF pupal thoraces, when the cell types in the ESO lineage have been determined. We observed that more than one internal cell is positive for Elav, a neuronal marker (Fig. 1, e–e′′′) and Prospero, a sheath cell marker (Fig. 1, f–f′′′) in mutant clones. In addition, we observe loss of Su(H), a marker for socket cells (Fig. 1, g–g′′′). Hence, the emergence of supernumerary neurons and sheath cells occurs at the expense of external cell types, i.e., socket and shaft cells. The transformation of cells within the mutant clones exhibits incomplete penetrance, i.e., in $2R11^{O4}$ homozygous mutant clones, ∼70% of the ESO cell clusters exhibit no Su(H) socket cells, whereas ∼40% of all Cut-positive ESO cells express Elav, as opposed to 25% in wild-type lineages. The incomplete penetrance of cell fate transformations has also been observed in other mutants that regulate Notch signaling, such as *sec15* and *spdo* (Hutterer and Knoblich, 2005; Jafar-Nejad et al., 2005).

To establish if Notch signaling is indeed impaired, we assessed the expression pattern of the transcription factor Tramtrack (Ttk). Ttk is expressed in the pIIa cell (signal receiving), but not in the pIIb (signal sending) cell (Guo et al., 1995), as a result of Notch signaling (Okabe et al., 2001; Pi et al., 2001). In mutant *2R11* clones, posterior cells do not express Ttk (Fig. 1, h–h′′′) similarly to their anterior pIIb sibling cells, indicating that Notch signaling is indeed affected and that pIIa cells have transformed into pIIb cells. Hence, *2R11* mutations affect Notch signaling during asymmetric divisions of ESO cells.

2R11 corresponds to CG15609, the fly homologue of Eps15 homology domain protein-binding protein 1

The *2R11* mutations were mapped by meiotic recombination using *P* elements (Zhai et al., 2003) followed by complementation tests with deficiencies and lethal alleles in the region of interest. All *2R11* alleles failed to complement *Df(2R)ED2751*, *Df(2R)Exel6065*, *Df(2R)ED3181* molecularly mapped deficiencies (Parks et al., 2004; Ryder et al., 2007; Cook et al., 2010). In addition, *2R11* alleles do not complement *P{lacW}l(2)k09837*, a lethal insertion of a *P* transposable element in the 5′ upstream regulatory region of the *CG15609* gene (Spradling et al., 1999), the "*P*" allele (Fig. 2 a). The lethality of *P{lacW}l(2)k09837* is due to the *P* element insertion because it is reversed upon precise excision of the *P* element. We also generated a deletion, $CG15609^{\Delta Ex24}$, by imprecise excision of the *P* element (Fig. 2 a). Flies homozygous for $CG15609^{\Delta Ex24}$ are lethal and fail to complement all

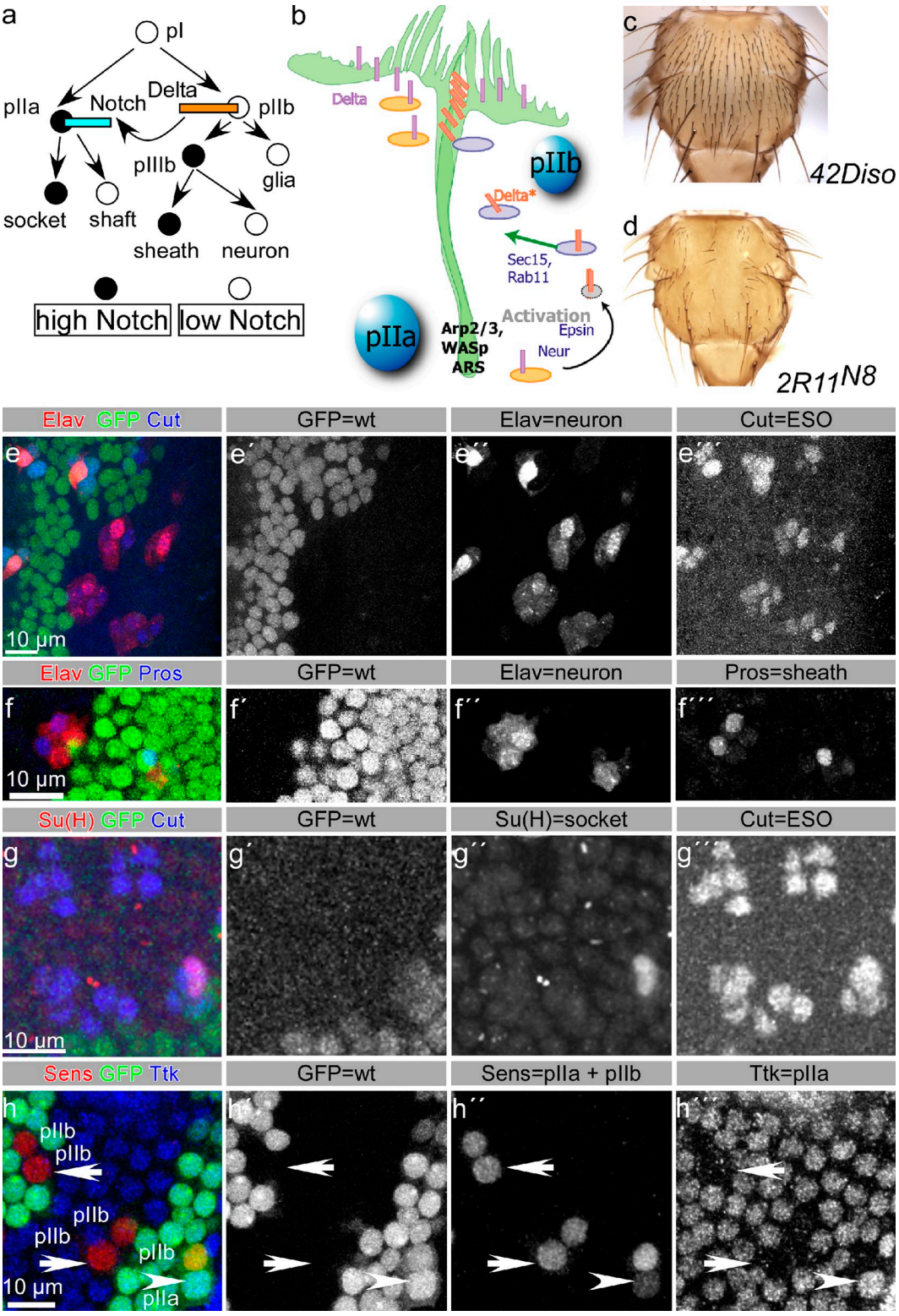

Figure 1. **2R11 alleles disrupt Notch signaling in the asymmetrically dividing thoracic ESO lineages.** (a) Diagram of the asymmetric divisions during development of the ESO lineage; black circles represent Notch signal–receiving cells, white circles represent Notch signal–sending cells. (b) A possible model for Notch signaling in asymmetrically dividing ESO lineages (adopted by Rajan et al., 2009). (c and d) Thoracic $y^{-/-}$ clones of the parental *42Diso* chromosome (c) or of the $2R11^{N8}$ allele (generated in a Minute background) (d). (e–g′′′) Analysis of different cell type markers of the ESO lineage at 24 h APF; pupal thoraces reveal that mutant ESO cells acquire erroneous cell fates. (e–e′′′) Supernumerary, elav-positive neurons arise in *2R11* negatively marked clones. (f–f′′′) Extra prospero–positive sheath and elav-positive neuron cells develop in *2R11* thoracic clones. (g–g′′′) Su(H)-positive socket cells are absent from *2R11* clones. In e-g′′′, cells of the ESO lineages are marked by Cut. (h–h′′′) Tramtrack-positive pIIa cells are absent from $dEHBP1^{A28}$ clones within pupal nota at 17 h APF, revealing that Notch signaling is affected within the mutant regions. pIIa and pIIb cells are stained for Sens. Arrows indicate mutant pIIa cells, and the arrowhead points to a wild-type pIIa cell. The alleles used in e–e′′′ and g–g′′′ are $dEHBP1^{O4}$. The alleles used in f–f′′′ and h–h′′′ are $dEHBP1^{A28}$. Bars, 10 µm.

other alleles (Fig. 2 d). The molecular lesions in the *2R11* mutants are either stop codons, deletions, or alterations in splice acceptor or splice donor sequences (Fig. 2 a), which are all predicted to cause truncated protein products of *CG15609* (Fig. 2 c). Finally, a genomic rescue construct spanning *CG15609* rescues all heteroallelic combinations (Fig. 2, a and d). Similarly, ubiquitous overexpression of the N-terminally FLAG-tagged cDNA isoform B rescued the lethality of *A28* and *O4* mutations over *Df(2R)Exel6065* (Fig. 2 d). These data demonstrate that *2R11* corresponds to *CG15609*.

CG15609 encodes the fly homologue of the human EHD protein-binding protein 1, an interacting partner of the Eps15 homology domain (EHD) 1 and 2 proteins (Guilherme et al., 2004a,b). In adipose cells and in the absence of insulin signaling, EHBP1 functions along with EHD2 in endocytosis of the GLUT4 glucose transporter, whereas upon insulin stimulation, EHBP1 and EHD1 mediate the recycling of GLUT4 back to the plasma membrane. In *Caenorhabditis elegans*, EHBP1 interacts with constitutively active Rab GTPase variants and is involved in the endocytic recycling of clathrin-independent cargoes (Shi et al., 2010), but it has not been implicated in Notch signaling in worms or vertebrates.

EHBP1 proteins contain multiple evolutionarily conserved domains (Fig. 2 b; Friedberg, 2010), i.e., an ∼200-aa-long, N-terminal C2-like lipid-binding domain (Zhang and Aravind, 2010), a middle calponin homology (CH) actin-binding domain (Gimona and Mital, 1998; Gimona et al., 2002; Korenbaum and Rivero, 2002), and a C-terminal, 200-aa-long, coiled coil region, which serves as a protein–protein interaction platform (Shi et al., 2010). In addition, the fly and mammalian EHBP-1 homologues have a putative CAAX box that may be involved in membrane anchoring, but this motif is not conserved in *C. elegans* (Shi et al., 2010).

To determine the expression pattern and subcellular localization of CG15609, we generated an anti-EHBP1 antibody against the full-length *Drosophila* protein. Anti-dEHBP1 fails to recognize the endogenous protein in either thoracic pupal clones homozygous for $dEHBP1^{O4}$ (Fig. 2, e–e′′′) or embryos that lack dEHBP1 ($dEHBP1^{\Delta Ex24}$; Fig. 2, f–g′′). dEHBP1 is expressed ubiquitously, but it is enriched in the embryonic central nervous system (CNS; Fig. 2, f–f′′). Moreover, in both epithelial thoracic cells (Fig. 2, e–e′′′) and embryonic CNS (Fig. 2, f–g′), dEHBP1 is mainly localized at the plasma membrane.

In summary, we have isolated loss-of-function mutations in *CG15609*, the fly homologue of EHBP1. Loss of dEHBP1 disrupts Notch signaling during asymmetric divisions in the ESO lineage, and dEHBP1 is ubiquitously expressed and localized mostly at or near the plasma membrane.

dEHBP1 is enriched at the actin-rich interface between the pII cells

To determine the subcellular localization of dEHBP1 we localized the protein with respect to an array of markers that delineate distinct plasma membrane subdomains along the apical–basal axis of epithelial cells (Humbert et al., 2003). Patj determines the apical region, Armadillo (Arm) and E-cadherin (Ecad) define the adherens junction, whereas Fasciclin III (FasIII) and Discs large (Dlg) mostly mark the lateral area of the plasma membrane (Fig. 3 h). dEHBP1 is present all around the plasma membrane of both pIIa and pIIb cells, but is especially enriched basally as well as laterally, at the interface of pIIa/pIIb cells, where it mostly colocalizes with FasIII and Dlg (Fig. 3, a–e′′′, g–j′′; and Fig. S1). The pIIa/pIIb interface is rich in actin filaments that assemble along the apico-basal axis and in apical microvilli in both cells, forming the ARS (Rajan et al., 2009). Because dEHBP1 is a putative actin-binding protein, we determined if dEHBP1 colocalizes with F-actin. Indeed, dEHBP1 colocalizes with F-actin at the pIIa/pIIb interface (Fig. 3, f–f′′ and i–j′′; and Fig. S1).

dEHBP1 exhibits a discontinuous, punctate pattern that likely reflects a dynamic, vesicular mode of trafficking (Fig. 3, g–g′′). To follow the trafficking of dEHBP1 in real time, we tagged dEHBP1 at its N terminus with mCherry. Expression of mCherry-dEHBP1 does not cause any cell fate transformations and is able to rescue the loss-of-function *dEHBP1* phenotypes (unpublished data). Overexpression of mCherry-dEHBP1 in ESO lineages results in its localization at the interphase of pII cells and in intracellular punctae, recognized also by the anti-dEHBP1 antibody (Fig. 3, i–j′′). Live imaging of ESO clusters at the one- and two-cell stage revealed that mCherry-dEHBP1 punctae are present in both pIIa/pIIb cells to an equal extent (Fig. 4, a–d; and Video 1). Moreover, mCherry-dEHBP1 concentrates transiently at the interface of pIIa/pIIb cells shortly after the division of the pI cell (Fig. 4, g and n).

To determine the nature of dEHBP1 punctae, we analyzed their colocalization with key Notch-signaling components, such as Spdo and Delta, which are also enriched at the interface of the pIIa/pIIb cells (Rajan et al., 2009; Tong et al., 2010; Benhra et al., 2011), as well as with a variety of subcellular markers including multiple Rab proteins, each identifying a discrete intracellular compartment (Fig. 4, Fig. S1; Stenmark, 2009). Hence, we assessed the colocalization of mCherry-dEHBP1 and Spdo-GFP in live imaging studies as well as endogenous dEHBP1 and Delta in immunofluorescent stainings. Although Spdo GFP is predominantly apical, whereas mCherry–dEHBP1 is enriched in subapical domains, we were able to detect colocalization of Spdo and dEHBP1 at the interface of the ESO cells (Fig. 4, g and i–k; and Video 2). However, we did not observe any colocalization of Spdo and dEHBP1 punctae in the cytoplasm (Fig. 4, l–r; Video 3). Similarly, we failed to see any colocalization between dEHBP1 and Delta in immunofluorescent stainings (Fig. 4, s–s′′′). Therefore, we conclude that dEHBP1 traffics to the interface of pII cells separately of Spdo and Delta vesicles. In addition, our live imaging analysis revealed only a rare and transient colocalization between dEHBP1 and Rab5-GFP or Rab11–GFP (unpublished data). dEHBP1 does not colocalize with Golgi markers, such as p120 kD, Syntaxin 16, and GM130, with the early endosome markers Avalanche and Rab5YFP, the late endosome markers Rab9YFP and Hook, the recycling endosome markers Rab11 and Rab11YFP, and the exocytic marker Rab10YFP (Fig. S1). Interestingly, we discovered that there is significant colocalization of dEHBP1 with Rab8YFP, a marker of exocytic vesicles that travel from trans-Golgi and through the recycling endosome to the plasma membrane (Huber et al., 1993; Ang et al., 2003; Henry and Sheff, 2008; Shi et al., 2010;

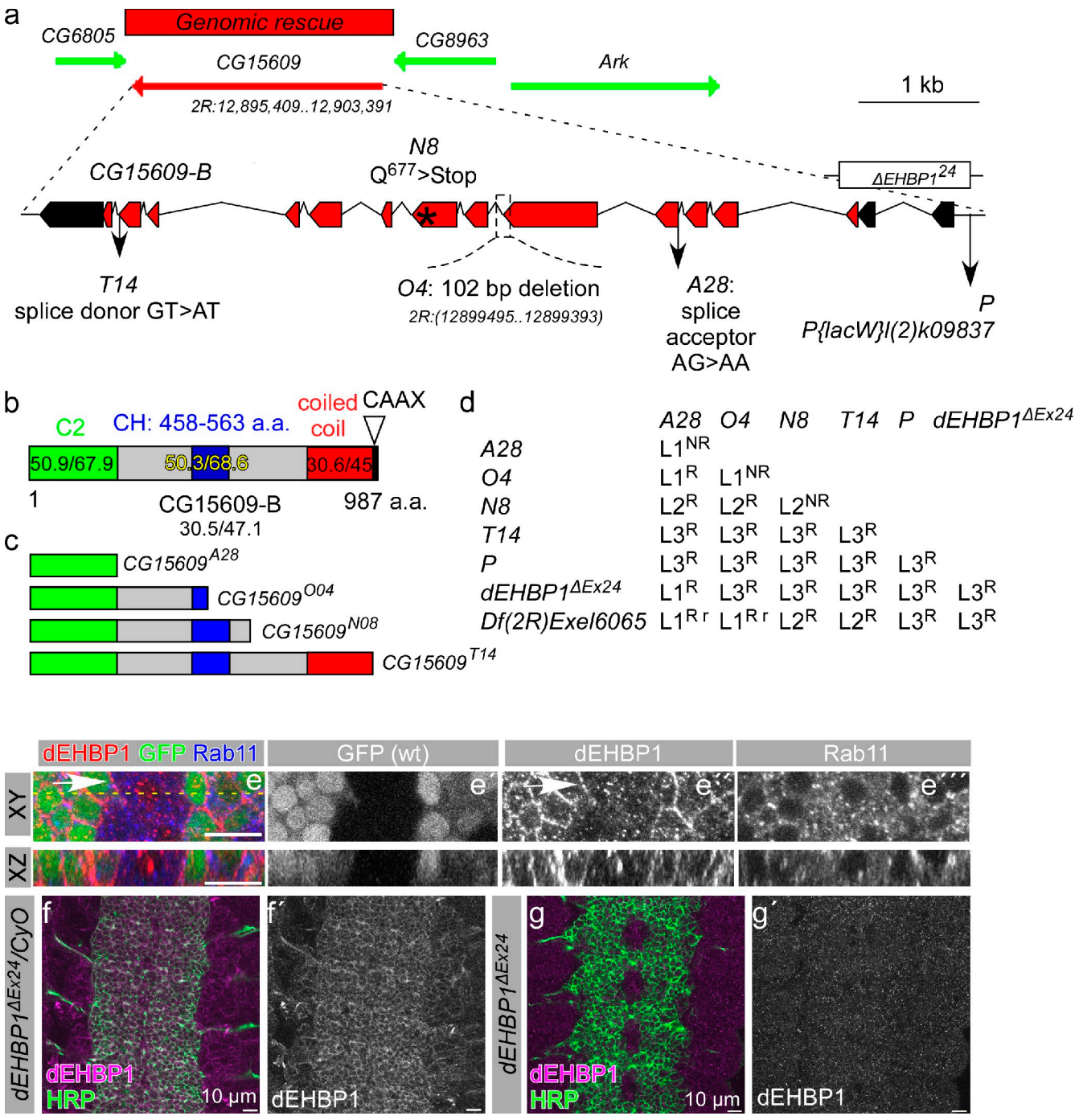

Figure 2. **2R11 alleles map to CG15609, the fly homologue of Eps15 homology domain containing protein-binding protein 1.** (a) Diagram of the genomic locus of *CG15609* (red arrow), the genomic rescue construct (red box), and the exon–intron structure of *CG15609* isoform B (red bars signify coding exons, black bars signify non coding exons), where the molecular lesions of *2R11* alleles are shown. *ΔEHBP1*^{ex24} is a deletion caused by imprecise excision of *P{lacW}l(2)k09837* (indicated as *P* allele). (b) Schematic representation of dEHBP1 protein structure. Percentages indicate identity/similarity between the fly and mouse homologues. C2 represents the lipid-binding domain and is colored in green, CH stands for calponin homology actin-binding domain and is colored in blue, coiled coil protein interaction domain is colored in red, and CAAX (C, cysteine; A, aliphatic; X, any amino acid) motif is shown as a triangle at the end of the protein sequence. a.a., amino acid. (c) The predicted structure of the dEHBP1 protein, in different mutant *2R11* alleles. (d) Lethal phase analysis of different mutations. NR, not rescued lethality; R, lethality rescued by genomic rescue; r, lethality rescued by cDNA, expressed ubiquitously by *tubGal4* driver. (e–e′′′) Anti-dEHBP1 fails to recognize the majority of the protein in pupal thoracic homozygous clones of *CG15609*^{O4}. Sections at both XY and XZ levels (indicated by yellow dashed line in e) are shown. Single-channel representations are shown in (e′) for GFP (wild-type region), (e′′) for dEHBP1, and (e′′′) for Rab11, which marks the recycling endosome. (f–g′) Anti-dEHBP1specifically recognizes dEHBP1 in embryonic CNS of control, balanced embryos (f–f′′) in comparison to CNS from homozygous mutant siblings (g–g′′). Bars, 10 μm.

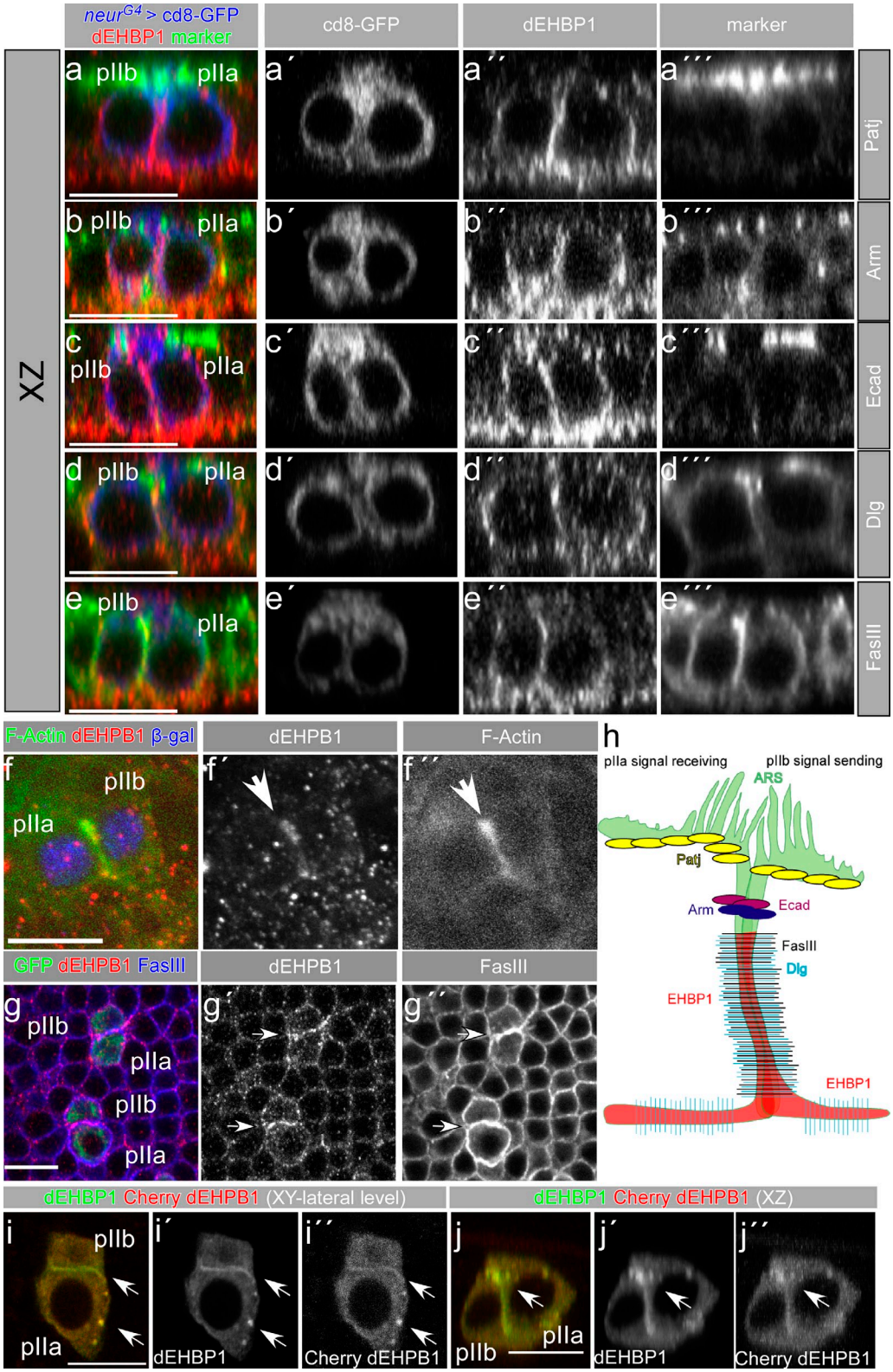

Figure 3. **dEHBP1 is enriched at the basolateral side of the plasma membrane and colocalizes with F-actin at the interface of pIIa and pIIb cells.** (a–e′′′) Analysis of the subcellular localization of dEHBP1 along the z axis with respect to various markers of apico-basal polarity in ESO cells (marked by *neur*^{Gal}*>UAS-cd8-GFP*), such as Patj (a–a′′′), Arm (b–b′′′), E-cad (c–c′′′), Dlg (d–d′′′), and FasIII (e–e′′′). (f–f′′) dEHBP1 colocalizes with F-actin at the interface of pIIa and pIIb cells, marked by the nuclear β-galactosidase (β-gal) in a *neur*^{A101} enhancer trap fly strain. (g–g′′) dEHBP1 exhibits a punctate pattern in thoracic epithelia. Arrows point to the enrichment of dEHBP1 at the interface of ESO cells (marked by *neur*^{Gal}*>UAS-cd8-GFP*). Bars, 10 µm. (h) Diagram depicting the relative localization of dEHBP1 with respect to markers of apico-basal polarity in ESO cells. Only the most prominent, basolateral expression of dEHBP1 with emphasis to the interface of ESO cells is shown, for the sake of clarity. (i–j′′) mCherry-dEHBP1, expressed in ESO lineages by *neur*^{Gal4}, localizes at the interphase of pII cells and within intracellular punctae, also recognized by the anti-dEHBP1 antibody. Sections are shown at the xy (i–i′′) as well as at the xz level (j–j′′).

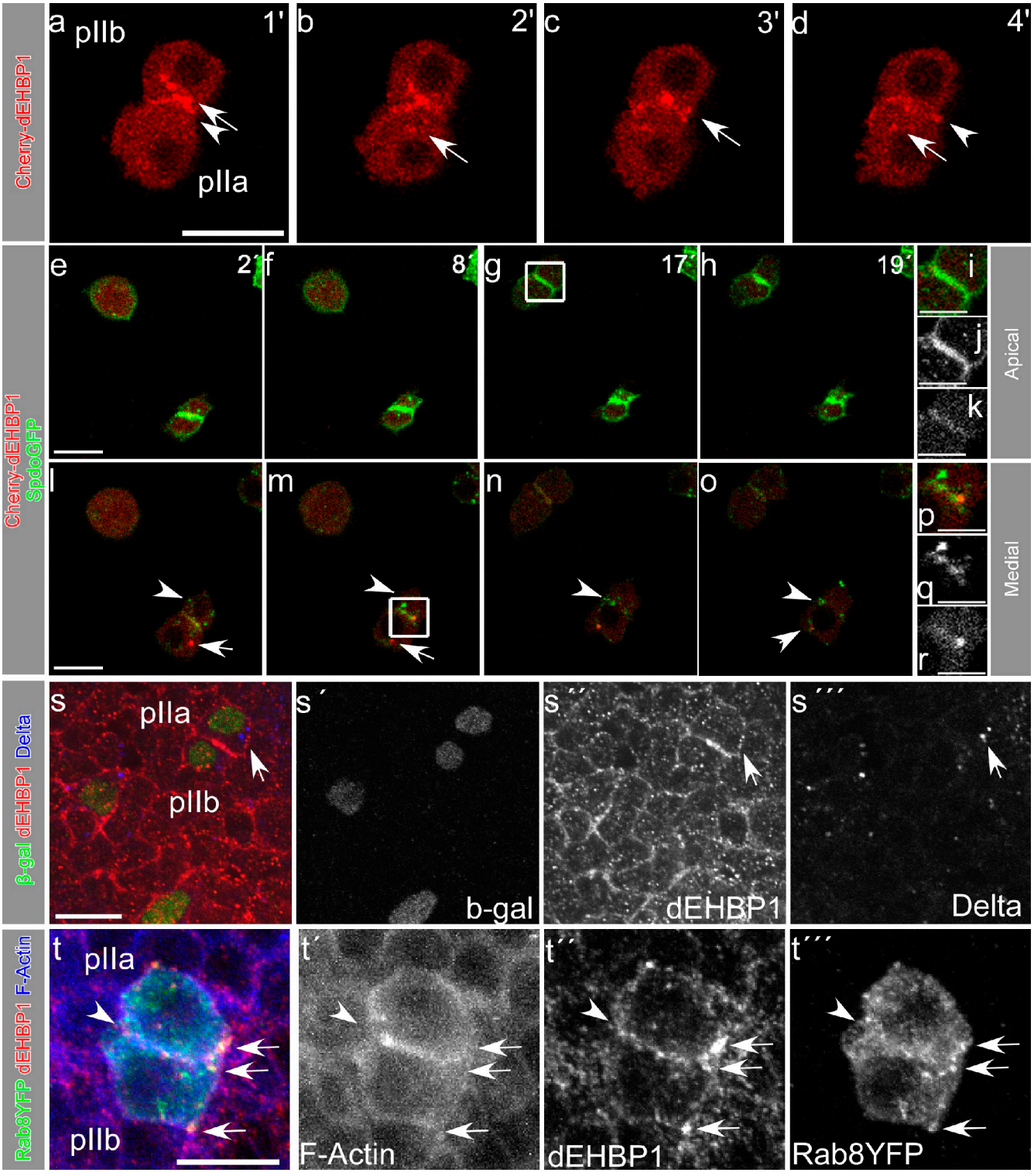

Figure 4. **dEHBP1 is transiently enriched at the interface of the pIIa/pIIb cells, where it partially colocalizes with Spdo.** (a–d) Still frames from Video 1 showing medial sections of pIIa/pIIb cells that contain mCherry-dEHBP1 in intracellular punctae, pointed by arrows, as well as the interface of the cells, indicated by arrowheads. Numbers at the top right corner indicate the minutes of live imaging. (e–k) Still frames from Videos 2 and 3 showing apical and medial sections of pIIa/pIIb cells, respectively, that express mCherry-dEHBP1 and Spdo-GFP, which colocalize along the interface of dividing pII cells toward the subapical regions (i–k). Numbers at the top right corner indicate the minutes of live imaging. (i–k) Magnification of the pIIa/pIIb cells included in the box in g. (l–r) mCherry-dEHBP1 (arrow) and Spdo GFP punctae (arrowheads) do not colocalize, but only at the interface of dividing pII cells (p–r). (p–r) Magnification of the pIIa/pIIb interface included in the box in m. Single-channel representations are shown in black and white for Spdo-GFP (q) and for mCherry-dEHBP1 (r). (s-s´´´) Single confocal sections of pIIa/pIIb cells of $neur^{A101}$ strain, marked by nuclear β-gal, indicate that dEHBP1 does not colocalize with Delta punctae (arrow). (t–t´´´) Rab8YFP, expressed in pII cells by $neur^{Gal4}$, colocalizes with dEHBP1 in vesicular structures as well as at the actin-rich interphase of pII cells, as indicated by the arrows and arrowheads, respectively. Bars: (p–r) 5 μm, (all others) 10 μm.

Das and Guo, 2011). Intriguingly, in nematodes, EHBP1 colocalizes with Rab10 and Rab8 GTPases, (Shi et al., 2010), two very similar GTPases in the secretory-recycling pathway (Pereira-Leal and Seabra, 2001; Das and Guo, 2011), and loss of EHBP1 phenocopies loss of *rab10* in endosomal recycling (Shi et al., 2010).

Even though we do not detect significant colocalization between dEHBP1 and Rab10 (Fig. S1), we addressed the role of *rab10* in asymmetric cell divisions by overexpressing dominant-negative *Rab10YFP* in ESO lineages, as there are no available alleles for *rab10*. We did not observe any defects in cell fate acquisition under these experimental conditions. Thus, loss of Rab10 function does not mediate the effect of dEHBP1 loss-of-function mutations. To address whether loss of *rab8* phenocopies loss of *dEHBP1*, we tested a $rab8^{1}$ allele. The molecular lesion in $rab8^{1}$ is a point mutation in the GTPase domain that alters the evolutionarily conserved serine at position 17 to phenylalanine (S17F). When $rab8^{1}$ is placed over a deficiency that uncovers the *rab8* locus, it results in pupal lethality. To perform clonal analysis, we recombined $rab8^{1}$ on a FRT80B chromosome. Loss of *rab8* in thoracic clones or overexpression of dominant-negative *Rab8YFP* in ESO lineages does not confer any cell fate phenotype. Therefore, loss of Rab8 function does not mediate the effect of *dEHBP1* loss-of-function mutations.

dEHBP1 regulates the intracellular levels of Spdo

The prominent accumulation of dEHBP1 at the interface of the pIIa/pIIb cells, where Spdo and Delta are targeted, strongly suggests that dEHBP1 may play a role in the localization of Spdo, Delta, or Notch. Indeed, loss of dEHBP1 causes a strong up-regulation of Spdo in the pI cell and its progeny (Fig. 5, Fig. S2, b–c′; and unpublished data). We did not observe the expansion of any of the other subcellular compartments, including ER, Golgi, and endosomal compartments (Fig. S2, a–e′). We were therefore unable to determine the specific subcellular compartment that contains Spdo. Importantly, we did not observe any aberrant localization of Delta or Notch using standard immunofluorescence assays (Fig. 5, b–e′). Neither did we observe any defects in the endocytosis of Notch (Fig. 5, f–f′′′). Furthermore, we did not observe any alterations in the apical–basal cellular polarity, as judged by the subcellular localization of Arm (unpublished data). In addition, the localization of Bazooka (Baz), a member of the Par complex that controls the anterior localization of the cell fate determinants Numb and Neur (Betschinger et al., 2003; Langevin et al., 2005; Roegiers et al., 2005; Wirtz-Peitz et al., 2008), occurs properly at the posterior cortex of the dividing pI cells (unpublished data). Finally, the cell fate determinants Numb and Neur form the proper crescent at the anterior cortex of the dividing pI cell, indicating that their asymmetric segregation occurs correctly in the absence of *dEHBP1* (Fig. S3, i–l′). In summary, the asymmetric segregation of key determinants occurs properly.

The aberrant up-regulation of Spdo may reflect its retention in the cytoplasm and a failure to reach the plasma membrane, as previously observed with the loss of *sec15* (Tong et al., 2010). We observed that, even in the absence of *dEHBP1*, Spdo is colocalized with FasIII at the plasma membrane, suggesting that it is not exclusively cytoplasmic (Fig. 5, g–j). It is however possible that certain parameters of Spdo trafficking may have been altered. For example, at this level of analysis, we cannot conclude whether Spdo is properly inserted in the plasma membrane. In addition, Spdo may linger in subcortical pools for a longer period of time and its access to Notch receptor may have been reduced, thus rendering its activation more difficult. Alternatively, the aberrant up-regulation of Spdo may negatively impact Notch signaling (Babaoglan et al., 2009). However, we and others have not observed any effects of Spdo overexpression upon cell fate acquisition in the ESO lineage (this paper; Jafar-Nejad et al., 2005; Tong et al., 2010).

To further dissect the function of *dEHBP1* in ESO lineage specification, we overexpressed a constitutively active form of atypical protein kinase C ($DaPKC^{\Delta N}$) in the wild-type and $dEHBP1^{-/-}$ thoracic clones. Overexpression of $DaPKC^{\Delta N}$ has been shown to result in retention of Spdo at the plasma membrane, conferring a partial Notch gain-of-function phenotype, i.e., generation of extra socket cells (Langevin et al., 2005; Roegiers et al., 2005). However, when we overexpressed $DaPKC^{\Delta N}$ in thoracic clones lacking *dEHBP1* we observed the same phenotype as in the cells that only lack *dEHBP1*, i.e., a Notch loss of function (Fig. S3, a, b, d, and e). Because constitutively active *DaPKC* results in Spdo localizing at the plasma membrane, we examined whether loss of *dEHBP1* suppresses the overexpression phenotype of $DaPKC^{\Delta N}$ by altering the subcellular localization of Spdo. We observe that Spdo still colocalizes with the membrane marker FasIII in $dEHBP1^{-/-}$ ESO lineages that overexpress constitutively active *DaPKC*, similarly to neighboring wild-type ones (Fig. S3, g–h′′). Therefore, dEHBP1 may affect other aspects of Notch signaling, such as the activity of the ligand Delta.

To corroborate our hypothesis, we examined whether loss of *dEHBP1* suppresses the Notch gain-of-function phenotype of the overexpressed activated Notch intracellular domain ($Notch^{NEXT}$). $Notch^{NEXT}$ functions in a ligand-independent, presenilin-dependent manner. We observe that loss of *dEHBP1* cannot suppress the supernumerary sockets that the overexpression of $Notch^{NEXT}$ causes, as judged by the macroscopic expression of enlarged socket structures within the thoracic clones and the supernumerary Su(H) socket cells in clones in pupal nota 24 h APF (Fig. S3, a, c, d, f, and m–n′′). Thus, *dEHBP1* functions upstream of the presenilin-mediated S3 cleavage of Notch. In conclusion, our data suggest that *dEHBP1* may not affect the activity of the Notch receptor, but most likely regulates other aspects of Notch signaling, such as the function of Spdo and/or the activity of the ligand Delta.

If dEHBP1 positively regulates the ability of Delta to signal, then loss of dEHBP1 would be epistatic to gain of function of Notch signaling, achieved by ectopic expression of Delta. Indeed, loss of *dEHBP1* results in the development of extra neurons in clones of cells despite the ectopic expression of an "activated" variant of Delta ligand, which is called $Delta^{R+}$ and is also dependent on ubiquitination and epsin-mediated recycling, similar to Delta (Fig. S3, o–o′′′; Wang and Struhl, 2004).

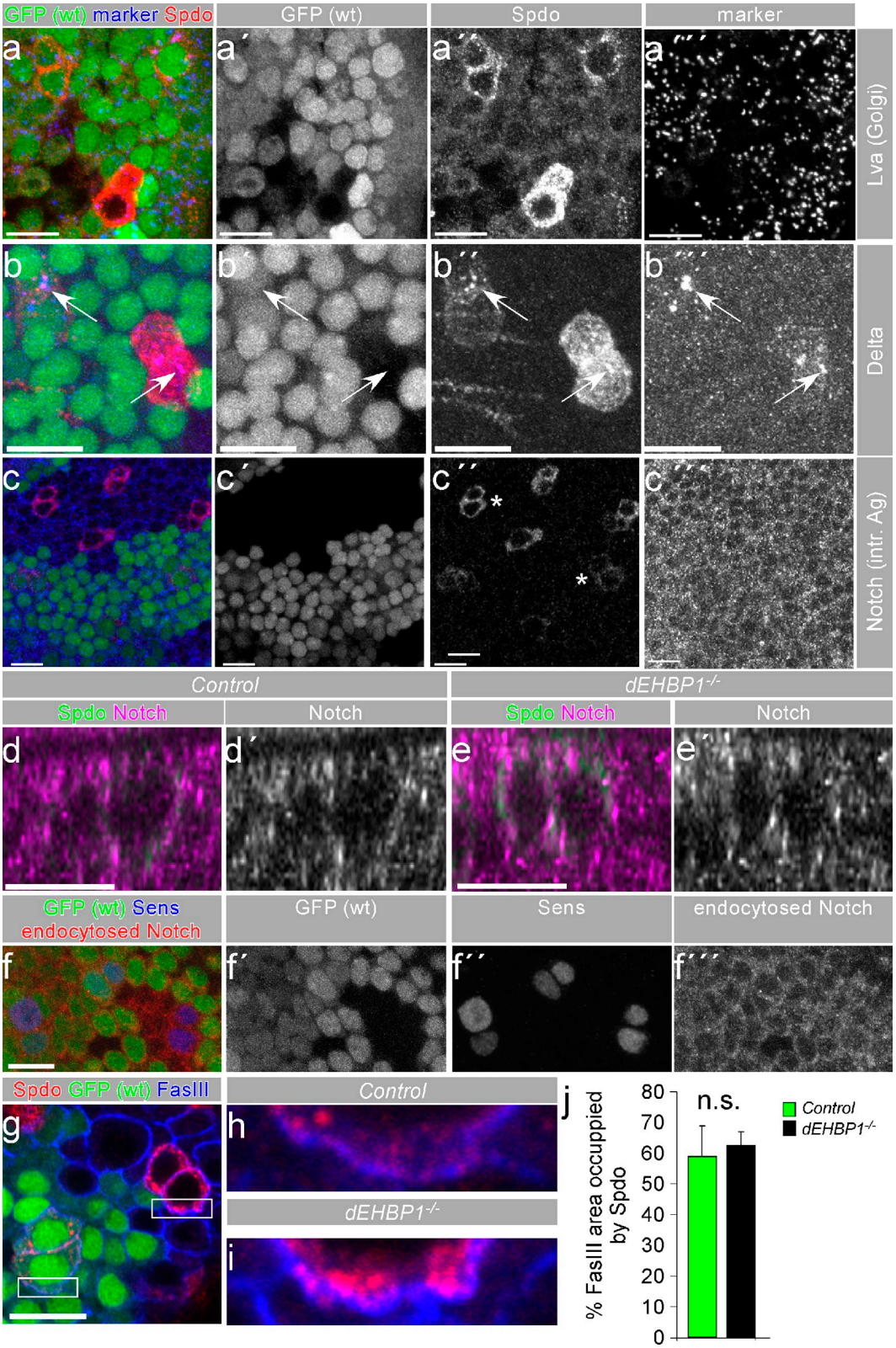

Figure 5. **Spdo is up-regulated in the absence of dEHBP1.** (a–b′′′) Spdo is up-regulated in *dEHBP1*$^{-/-}$ ESO cells but not restricted in a Lva-positive Golgi compartment (a–a′′′) and not accompanied by a similar accumulation of Delta (b–b′′′). Arrows indicate to the colocalization of intense Spdo punctae with Delta in both wild-type and mutant cells. (c–c′′′) Spdo is up-regulated in *dEHBP1*$^{-/-}$ ESO cells, but not accompanied by accumulation of Notch (d–e′) Notch does not display aberrant localization along the xz axis in ESO clusters, indicated by the asterisks in c′′. (f–f′′′) Endocytosis of Notch is not altered in the absence of dEHBP1. (g–i) Spdo is up-regulated in *dEHBP1*$^{-/-}$ ESO cells, but not excluded from the FasIII-positive part of the plasma membrane, as shown in single confocal sections. Magnification of parts of the plasma membrane, included in the boxed regions in g, are shown for a wild-type, GFP-positive ESO cluster (h) and for mutant, GFP-negative, ESO clusters (i). (j) Quantification of the FasII-positive area that is occupied by Spdo in control and *dEHBP1*$^{-/-}$ ESO clusters indicates that Spdo is able to reach the plasma membrane in the absence of dEHBP1. Bars, 10 μm.

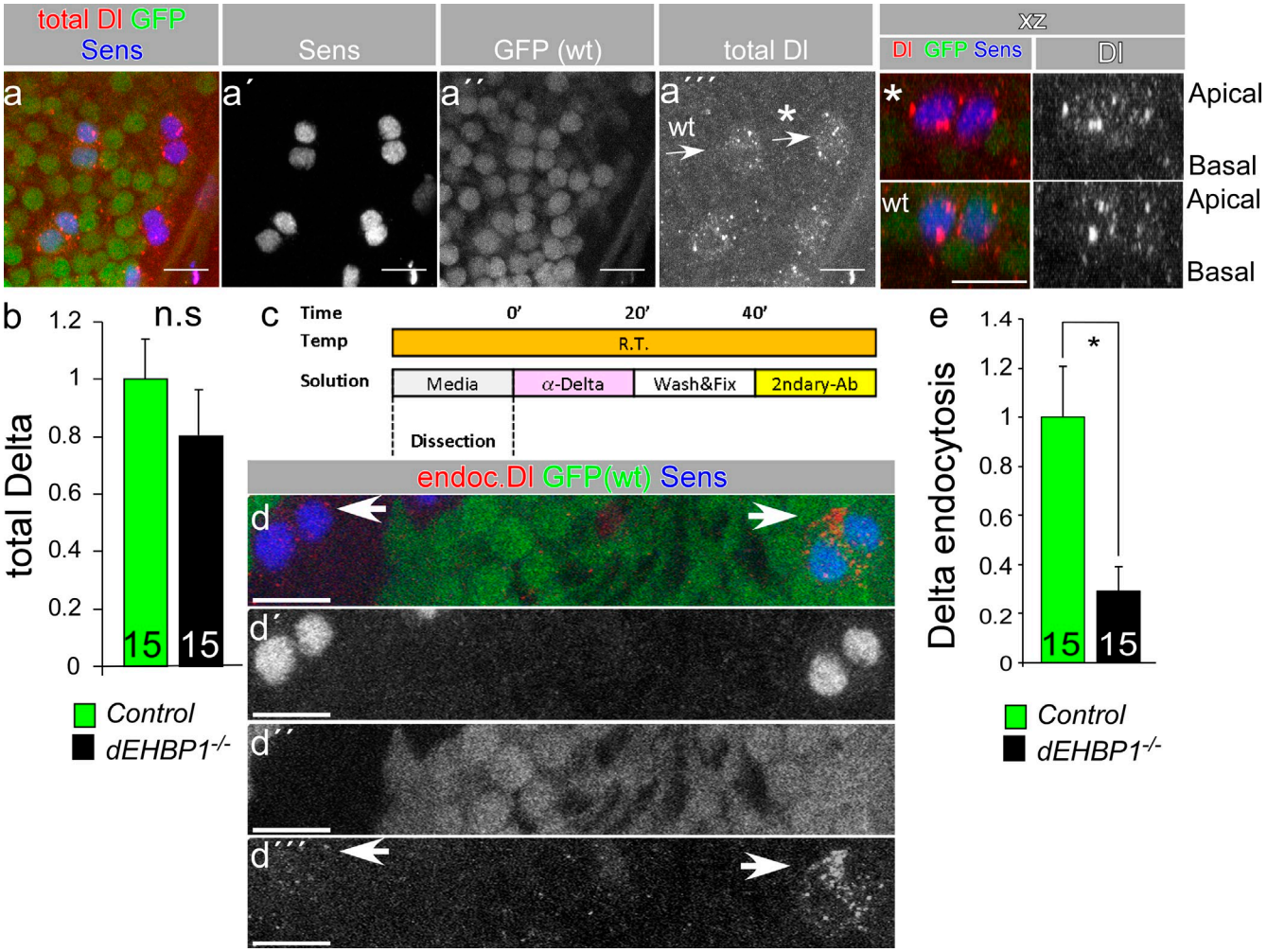

Figure 6. **Delta endocytosis is impaired in the absence of dEHBP1.** (a–a′′′) The total amount of Delta is not affected upon loss of *dEHBP1*. The asterisk marks the *dEHBP1*$^{-/-}$ cell cluster, and wt stands for the wild-type control cluster. (b) Normalized quantification of levels of total Delta in wild-type (green bars) and *dEHPB1*$^{-/-}$ (black bars) ESO clusters. Numbers at the base of the bars represent the number of ESO clusters used for quantification; n.s., not significant. (c) Schematic representation of the Delta endocytosis assays; R.T., room temperature. (d–d′′′) Delta endocytosis is impaired under conditions of loss of function of *dEHBP1*. Arrows point to the Delta punctae detected in the endocytosis assay. Few, small punctae are still seen in the mutant ESOs, suggesting that endocytosis is not completely abolished. (e) Normalized quantification of endocytosed Delta (in d–d′′′) in wild-type (green bars) and mutant (black bars) ESO two-cell clusters. Numbers at the base of the bars represent the number of ESOs of two-cell clusters used for quantification. *, $P < 0.05$.

These results suggest that *dEHBP1* affects the output of Notch signaling even upon overexpression of Delta^{R+}, because it may affect the function of Spdo and/or it affects the trafficking and signaling capacity of Delta^{R+}.

dEHBP1 regulates trafficking of Delta

The localization of Delta is unaffected in the absence of *dEHBP1* in immunofluorescent stainings of pupal thoraces at 17 h APF using standard immunofluorescence stainings (Fig. 6, a–b). These stainings are based on permeabilizing conditions that reveal the localization of both extracellular and intracellular Delta (Fig. 6, a–b). It has been proposed that Delta is endocytosed mainly at the basal side of ESO lineages in a *neur*-dependent fashion (Benhra et al., 2011). Upon endocytosis, it is then transcytosed to the apical side, where it will interact with Notch (Benhra et al., 2011). To assess whether Delta endocytosis is affected, we performed Delta endocytosis assays (Le Borgne and Schweisguth, 2003). In brief, extracellular Delta molecules are conjugated with anti-Delta antibodies under nonpermeabilizing conditions over a 20-min period at room temperature, allowing uptake in the cells. The internalized complexes of Delta antibodies are then detected by fluorescent secondary antibodies (Fig. 6 c). Interestingly, uptake of Delta antibody complexes is dramatically impaired in *dEHBP1*$^{-/-}$ clusters (Fig. 6, d–e), suggesting that either endocytosis is impaired or that the abundance of Delta molecules present on the cell surface is much decreased.

The total pool of Delta present at the membrane consists of a pool of Delta that is initially delivered to the plasma membrane, as well as a pool of Delta that is recycling back to the ARS at the interface of pIIa and pIIb cells upon endocytosis (Emery et al., 2005; Jafar-Nejad et al., 2005; Rajan et al., 2009; Benhra et al., 2011). To assess Delta trafficking, we performed Delta pulse-chase assays (Fig. 7 a). In brief, pupal thoraces were incubated under nonpermeabilizing conditions with anti-Delta antibodies over a 30-min period on ice, to block endocytosis.

This allows anti-Delta-antibodies to bind to Delta at the cell surface. If the tissue is fixed immediately upon incubation with the antibodies, we can estimate the total amount of Delta that is accessible by the antibodies and therefore, the total membrane-associated pool of Delta. We define this time point as 0 min. If the tissue is fixed after chase for 60 min at room temperature we can estimate the rate of uptake. We define this as time point 60 min. We find that in *dEHBP1*$^{-/-}$ cells, the amount of Delta is reduced both at time point 0 and 60. These data indicate that exocytosis of Delta is impaired in the absence of *dEHBP1* (Fig. 7, b–c′, g).

To corroborate our conclusions, we analyzed the distribution of exocytosed Delta by detecting extracellular Delta in ESO clusters under nonpermeabilizing conditions: the tissue is fixed in the absence of detergent and incubated overnight with anti-Delta. The data show that in *dEHBP1*$^{-/-}$, extracellular Delta is severely decreased, suggesting that exocytosis of Delta is indeed impaired. Some of the remaining Delta is localized basally (Fig. 7, d–f′′′ and h). These data suggest that Delta exocytosis is impaired and that trafficking from the basal to the apical membrane is severely disrupted.

dEHBP1 localization is controlled by Sec15, and dEHBP1 physically interacts with Rab11 and Sec15

The enrichment of dEHBP1 at the signaling interface of pIIa/pIIb cells correlates with the failure of Delta to localize at the interface in *dEHBP1*$^{-/-}$ cells. Therefore, *dEHBP1* may control the abundance and/or subcellular localization of components that affect Delta localization at the ARS, such as Rab11 and its effector Sec15 (Zhang et al., 2004). We found that *dEHBP1* does not affect the subcellular localization of Rab11 or Sec15 (Fig. S2, e–f′). Alternatively, dEHBP1 may affect the integrity of ARS. However, the umbrella-shaped morphology of the ARS is undisturbed in the absence of dEHBP1 (Fig. S2, g–i).

Conversely, we asked whether any of the components that regulate Delta recycling to the ARS are important for the localization dEHBP1, such as *Arp3* and *sec15*. Because dEHBP1 is a putative actin-binding protein, we first examined whether disruption of the ARS results in mislocalization of dEHBP1 and consequently whether it confers accumulation of Spdo. We found that in the absence of *Arp3* activity (Rajan et al., 2009), dEHBP1 is correctly localized and Spdo fails to accumulate within the ESO cluster (unpublished data). Thus, loss of function of *Arp3* does not affect the subcellular localization and function of dEHBP1. As loss of *rab11* is cell lethal (Emery et al., 2005; Banks et al., 2011), we asked whether loss of *sec15* leads to mislocalization of dEHBP1. As shown in Fig. 8 a, the subcellular localization of dEHBP1 is severely disrupted in the absence of *sec15* because dEHBP1 accumulates at the basal side in both epithelial cells as well as within ESO lineages, where it colocalizes with Delta in the same subcellular compartment (Fig. 8, a–c′′). Thus, both dEHBP1 and Delta depend on Sec15 for their proper intracellular trafficking.

The dependence of dEHBP1 subcellular distribution on *sec15* prompted us to assess if dEHBP1 and Sec15 interact physically. Indeed, dEHBP1 coimmunoprecipitates with Sec15 from whole-cell extracts of transiently transfected S2 cells (Fig. 8 f). The physical interaction between dEHBP1 and Sec15 may reflect their colocalization in vivo. Indeed, Sec15-GFP colocalizes with dEHBP1 at the interface of pII cells in ESO clusters (Fig. 8, d–d′′) and within punctate structures (Fig. 8, e–e′′). Taken together, these results suggest that Sec15 regulates the recycling of Delta and the subcellular distribution of dEHBP1, with which it physically interacts and colocalizes in vivo.

We attempted to map the domain of dEHBP1 that is necessary for interaction with Sec15 by in vitro GST pull-down assays unsuccessfully, suggesting that dEHBP1 may interact with Sec15 via other protein intermediates. One possibility is that dEHBP1 may interact with Sec15 via its interaction with Rab11 GTPase, whose effector is Sec15. However, we were unable to observe any direct interaction of dEHBP1 and Rab11 in in vitro GST pull-down assays (Fig. 8 g) or in yeast two-hybrid experiments (not depicted). To further examine the possibility of physical interactions between dEHBP1 and Rab11, we performed coIP from S2 whole-cell extracts that were transiently transfected with wild-type or constitutively active or dominant-negative HA-tagged variants of Rab11 and FLAG-dEHBP1. As shown in Fig. 8 h, dEHBP1 interacts strongly with the dominant-negative variant of Rab11 and very weakly with the wild-type or constitutively active variant of Rab11. As dominant-negative forms of Rab proteins mimic the GDP-bound inactive state, these data suggest the possibility that dEHBP1 may act at a step just before the activation of Rab11. In conclusion, dEHBP1 depends on Sec15 for its subcellular localization, and it can physically interact with Rab11 and Sec15. We envision that dEHBP1 may act along with Rab11 and Sec15 during the trafficking of Delta-bearing vesicles toward the ARS.

Discussion

In the present study, we describe the identification of *dEHBP1* as a novel, positive regulator of Notch signaling in asymmetrically dividing cells in the ESO lineage in *Drosophila*. In the absence of *dEHBP1,* external cell types, such as socket and shaft cells, are transformed into internal cell types, i.e., neuron and sheath cells, one of the hallmarks of loss of Notch signaling. EHBP1 has been previously studied in mammalian cell culture systems and in vivo in *C. elegans*. In mammalian adipocytes, EHBP1 affects endocytosis and recycling of the glucose transporter GLUT4 in the context of insulin signaling, depending on its interaction via the NPF motifs present in its N-terminal region with EHD2 or EHD1, respectively (Guilherme et al., 2004a,b). However, the fly and worm EHBP1 lack the NPF motifs (unpublished data and Shi et al., 2010), suggesting that the EHD–EHBP1 interaction may have emerged later in evolution. In *C. elegans*, EHBP1 was shown to impair *rab10*-mediated endocytic recycling of clathrin-independent endocytosed cargoes, such GLR-1 glutamate receptor (Shi et al., 2010). Here, we show for the first time that *dEHBP1* is required in the exocytosis and recycling of Delta, a ligand of the Notch receptor. Notch signaling defects were not reported in *C. elegans ehbp1* mutants.

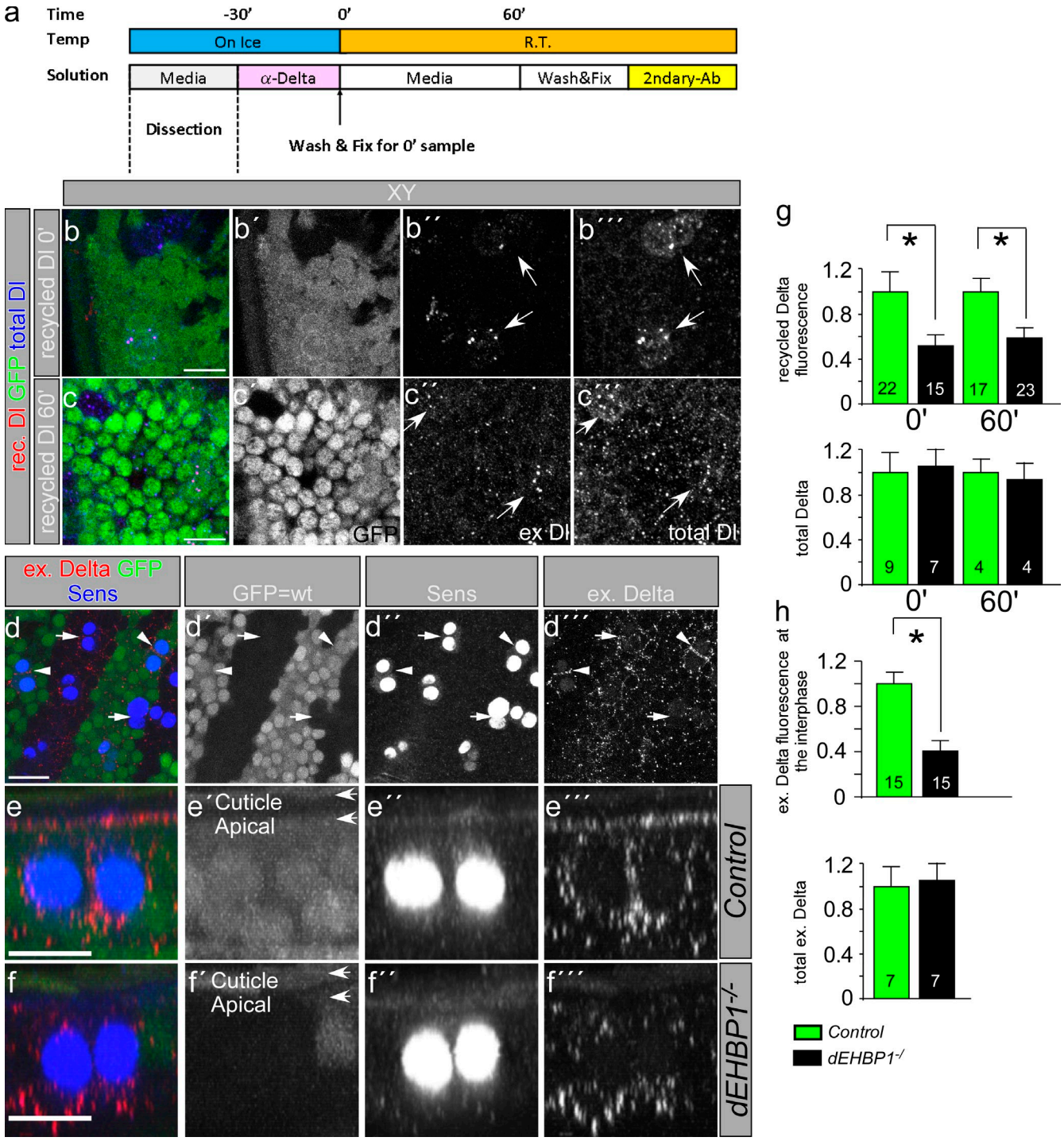

Figure 7. **Delta localization at the signaling interface of the pIIa/pIIb cells is impaired in the absence of dEHBP1.** (a) Schematic representation of the Delta pulse-chase assays. R.T., room temperature. (b–c′′′) Delta is reduced in *dEHBP1*$^{-/-}$ pIIa and pIIb cells at 0-min time points (b–b′′′) and at the 60-min time point (c–c′′′) in pulse-chase assays, as shown in xy projections. In b′′, b′′′, c′′, and c′′′, arrows point to the interface of mutant and wild-type two-cell ESO clusters, respectively. (d–f′′′) Extracellular Delta is reduced in *dEHBP1*$^{-/-}$ pIIa and pIIb cells, as shown in xy projections in d–d′′′, where arrows and arrowheads point to the interface of mutant and wild-type two-cell ESO clusters, respectively. Analysis of extracellular Delta in projections along the z axis of wild-type thoracic (e–e′′′′) and mutant (f–f′′′) thoracic clusters, respectively, reveal that Delta is severely reduced at the interface of the pIIa and pIIb cells and that it is mainly localized basally. (g) Normalized quantification of pulse-chased and total Delta at 0- and 60-min time points in wild-type (green bars) and mutant (black bars) ESO two-cell clusters. (h) Normalized quantifications of extracellular Delta at the interphase of wild-type (green bars) and mutant (black bars) pII cells, as well as total extracellular Delta throughout wild-type (green bars) and mutant (black bars) thoracic epithelia. The numbers at base of the bars in g and h represent the total number of clusters used for quantification of Delta. n.s., not significant; *, $P < 0.05$. Bars, 10 µm.

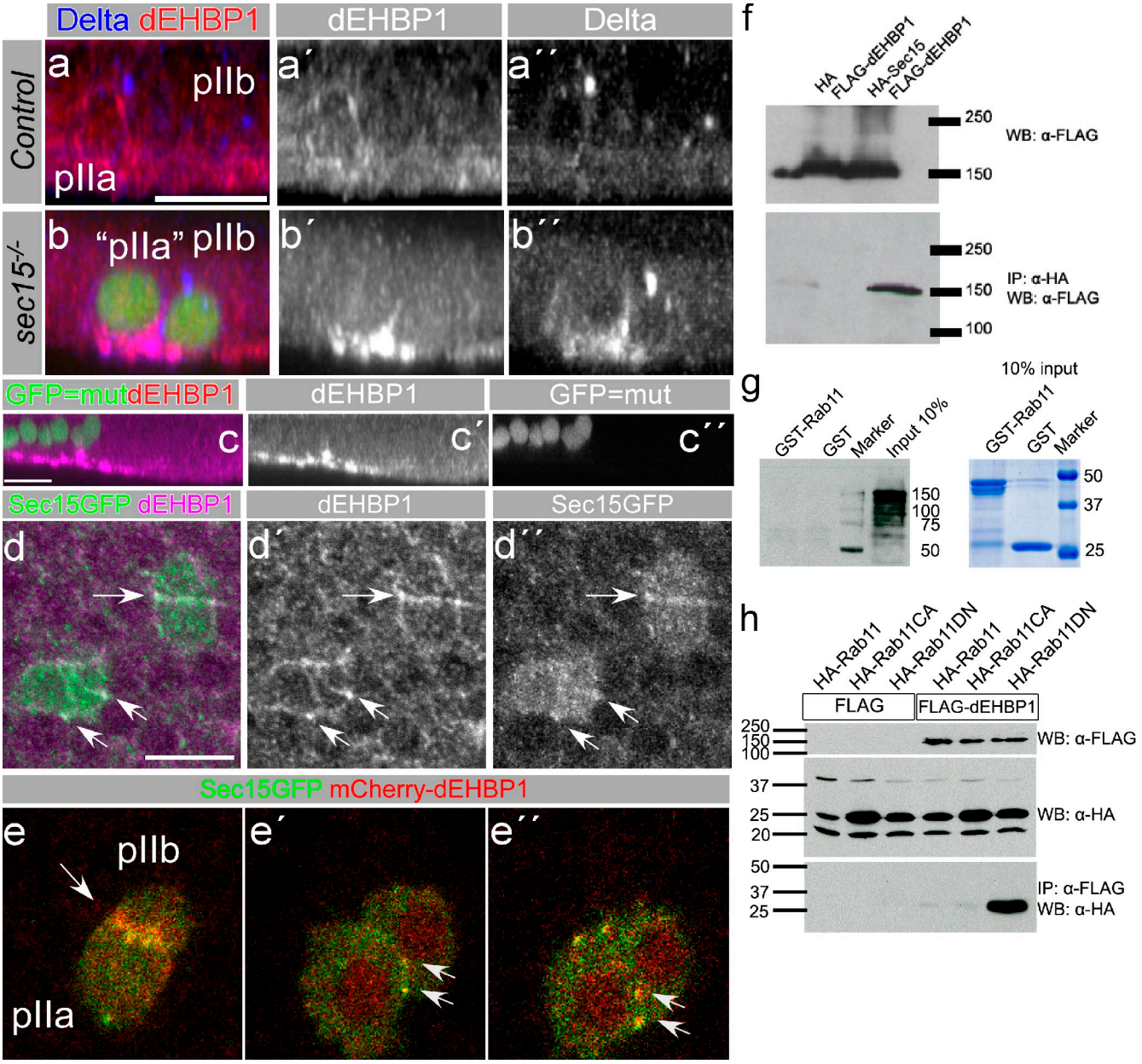

Figure 8. **dEHBP1 accumulates with Delta in the absence of Sec15 and it physically interacts with Sec15 and Rab11.** (a–b′′) xz projection of single ESO clusters within thoracic epithelia, which are wild-type (a–a′′) or homozygous mutant for *sec15* (b–b′′, positively marked by the expression of GFP), reveals that dEHBP1 accumulates basally along with Delta in the absence of *sec15*. (c–c′′) XZ projection of thoracic epithelia, shown in a–b, which contain homozygous mutant cells for *sec15* (c′′, positively marked by the expression of GFP), reveals that dEHBP1 accumulates basally in all epithelial cells in pupal thoraces in the absence of *sec15*. (d–d′′) Sec15-GFP, overexpressed by $neur^{Gal4}$, and dEHBP1 colocalize in ESO clusters at the interface of the progeny, as indicated by the arrows. Single-channel representations for dEHBP1 (d′) and Sec15-GFP (d′′) are shown in black and white. (e–e′′) Sec15-GFP and mCherry-dEHBP1 overexpressed by $neur^{Gal4}$ colocalize in ESO clusters. (f) HA-Sec15 and FLAG-dEHBP1 coimmunoprecipitate from whole-cell lysates of transiently transfected S2 cells. (g) GST-Rab11 does not interact with in vitro–translated dEHBP1. 10% input of the proteins used for the GST pull-down were analyzed by Coomassie stain to ensure the integrity and equal amounts of GST proteins. (h) dEHBP1 interacts weakly with wild-type and constitutively active Rab11 variants, but strongly with dominant-negative Rab11 in coIP experiments from S2 cells. Bars, 10 µm.

Therefore, it would be interesting to investigate whether EHBP1 and its homologues play an evolutionarily conserved role of EHBP1 in Notch signaling.

dEHBP1 is a ubiquitous protein that is associated with the plasma membrane, enriched at the lateral and basal surface of pII cells, where it colocalizes with F-actin. Our live imaging with mCherry-dEHBP1 and immunofluorescent stainings with anti-dEHBP1 antisera also reveal dEHBP1-positive, punctate, intracellular structures within ESO lineages. An extensive analysis with a diverse array of intracellular markers revealed that these punctae colocalize with Rab8, indicating their exocytic nature (Huber et al., 1993; Ang et al., 2003). Importantly, in *C. elegans*, EHBP1 physically interacts and colocalizes with Rab8 and Rab10, and controls the recruitment of Rab10 in recycling endosomal structures (Shi et al., 2010). However, in our studies, overexpression of dominant-negative forms of Rab10 or Rab8 in the ESO

lineages as well as thoracic clones of a newly identified Rab8 loss-of-function allele do not confer any cell fate phenotypes. Furthermore, we have not detected any interaction between dEHBP1 and Rab8 or Rab10 in a yeast two-hybrid analysis. Therefore, we believe that loss of either Rab8 or Rab10 function does not underlie the dEHBP1 mutant phenotypes we describe.

Notably, many key players that affect cell polarity or mark subcellular compartments, including Arm, Rab11, Sec15, and F-actin, are not affected by the loss of *dEHBP1*. In addition, cell fate determinants Numb and Neuralized are correctly segregated upon asymmetric cell division in *dEHBP1* mutant cells. However, loss of *dEHBP1* specifically affects the abundance and localization of Spdo, a regulator of Notch signaling in asymmetrically dividing ESO cells, and the exocytosis and trafficking of Delta.

Spdo facilitates reception of Notch signal at the plasma membrane of the signal-receiving cell (Dye et al., 1998; O'Connor-Giles and Skeath, 2003; Benhra et al., 2010; Tong et al., 2010). Therefore, accumulation of Spdo in *dEHBP1*$^{-/-}$ ESO clusters and its presence in the plasma membrane should result in a Notch gain of function, instead of the loss-of-function phenotype we observe. We and others have not observed any effects of Spdo overexpression upon cell fate acquisition in the ESO lineage (this paper; Jafar-Nejad et al., 2005; Tong et al., 2010). Alternatively, the accumulation of Spdo in the absence of *dEHBP1* in these cells may reflect defects in its trafficking and membrane localization, which render the activation of Notch signaling more difficult.

dEHBP1 mutations cannot suppress the gain of function phenotype of overexpressed ligand-independent, activated Notch intracellular domain. In addition, dEHBP1 does not affect the steady-state levels of Notch protein, as well as its endocytosis. Therefore, we conclude that dEHBP1 functions at a level upstream of presenilin-mediated S3 cleavage of Notch during reception of the signal. Although we cannot exclude that *dEHBP1* functions in the signal-receiving cell, where it may control the trafficking and localization of Spdo, we conclude that *dEHBP1* also functions in the sending of the signal. Our conclusion is based on the fact that *dEHBP1* mutations are able to suppress the gain of function of Notch phenotype conferred by the overexpression of *DaPKC*$^{\Delta N}$. Overexpressed constitutively active *DaPKC*$^{\Delta N}$ places Spdo at the plasma membrane, enabling the activation of Notch signaling (Langevin et al., 2005; Roegiers et al., 2005). We find that upon loss of *dEHBP1*, Spdo is still found at the plasma membrane under conditions of overexpression of *DaPKC*$^{\Delta N}$. Therefore, the suppression of the overexpression phenotype of *DaPKC*$^{\Delta N}$ by loss of dEHBP1 may be because of other defects, such as loss of the ability of Delta to signal (Fig. S3). Furthermore, loss of *dEHBP1* leads to development of additional neurons despite the concomitant ectopic expression of Delta^{R+}, a variant of Delta, in clones within pupal nota at 36 h APF. Because the steady-state levels of Delta are not affected in *dEHBP1*$^{-/-}$ ESO lineages, we examined whether *dEHBP1* affects Delta trafficking in the signal-sending cell. Upon loss of *dEHBP1*, the abundance of Delta at the cell surface is significantly reduced, suggesting that exocytosis is defective. Importantly, most of the remaining extracellular Delta protein localizes at the basal side of the signal-sending cell. This suggests that in addition to affecting exocytosis of Delta, dEHBP1 may also play a role in basal-to-apical trafficking of Delta. This leads to a reduced level of Delta at the signaling interface, which interferes with proper Notch signaling in the cell receiving the signal. Although our results do not exclude a possible role of dEHBP1 in other aspects of Delta trafficking, such as endocytosis, reduced exocytosis of Delta should mask an endocytic defect in our assays. The enrichment of dEHBP1 in the basal and lateral area of the plasma membrane, its colocalization with F-actin at the ARS at the interface of the pIIa and pIIb cells, the reduction of Delta exocytosis in mutant cells, and the absence of Delta at the interface and the apical surface of the ESO cluster in mutant cells indicate a role of dEHBP1 in the Sec15/Rab11 recycling pathway. Indeed, the colocalization of dEHBP1 and Delta in *sec15*$^{-/-}$ ESO lineages implies that the exocyst component, Sec15, controls exocytosis of Delta, Spdo, and dEHBP1 to the apical plasma membrane through a common compartment. Because loss of *dEHBP1* does not affect the localization of either Rab11 or Sec15, we conclude that *sec15* lies more upstream in the trafficking pathway regulating the localization of multiple components, while dEHBP1 functions during the later stages of intracellular trafficking. Furthermore, the physical interaction between dEHBP1 and Sec15 as well as Rab11 suggest a mechanism how dEHBP1 may regulate the membrane localization of Delta via its interaction with Sec15 and Rab11 at the pII cells interface, even though such interaction was detected under transient overexpression conditions. We propose that dEHBP1 is an adaptor of the Rab11/Sec15-positive, Delta-bearing vesicles required for exocytosis (Fig. 9).

The identification of dEHBP1 provides further compelling evidence that the exocytosis and recycling pathway of Delta during asymmetric divisions is tightly regulated (Emery et al., 2005; Jafar-Nejad et al., 2005; Rajan et al., 2009). The recycling pathway of Delta appears to be context dependent, i.e., it is not required in all cells that use Notch signaling (Windler and Bilder, 2010; Yamamoto et al., 2010; Banks et al., 2011). Still, the discovery of dEHBP1 as a novel player in Notch signaling provides the opportunity to test its role in Notch-related neurobiological behaviors, such as sleep and addiction (Kaun et al., 2011; Seugnet et al., 2011), as well as in Notch-related diseases, as for example in Wiskott-Aldrich syndrome, an immunodeficiency characterized by abnormal differentiation and function of T cell lineages (Cotta-de-Almeida et al., 2007; Radtke et al., 2010; Thrasher and Burns, 2010). Furthermore, because the anthrax toxins lethal factor (LF) and edema factor (EF) inhibit the Sec15/Rab11-dependent Delta-recycling pathway in flies and endothelial cells (Guichard et al., 2010), it would be interesting to hypothesize whether they target dEHBP1 to mediate their toxicity.

Materials and methods

Fly strains, genetics, and transformation

The following stocks were used: *yw;FRT42D, yw;FRT42DdEHBP1*^{A28}*/CyO, yw;FRT42DdEHBP1*^{O4}*/CyO, yw;FRT42DdEHBP1*^{N08}*/CyO, yw;FRT42D-dEHBP1*^{T14}*/CyO, dEHBP1*$^{\Delta Ex24}$*/CyO, yw; CyO, H{w[+mC]=PDelta2-3}HoP2.1/Bc*^{1}*; P{lacW}l(2)k09837/CyO, Df(2R)ED2751/CyO, Df(2R)Exel6065/CyO,*

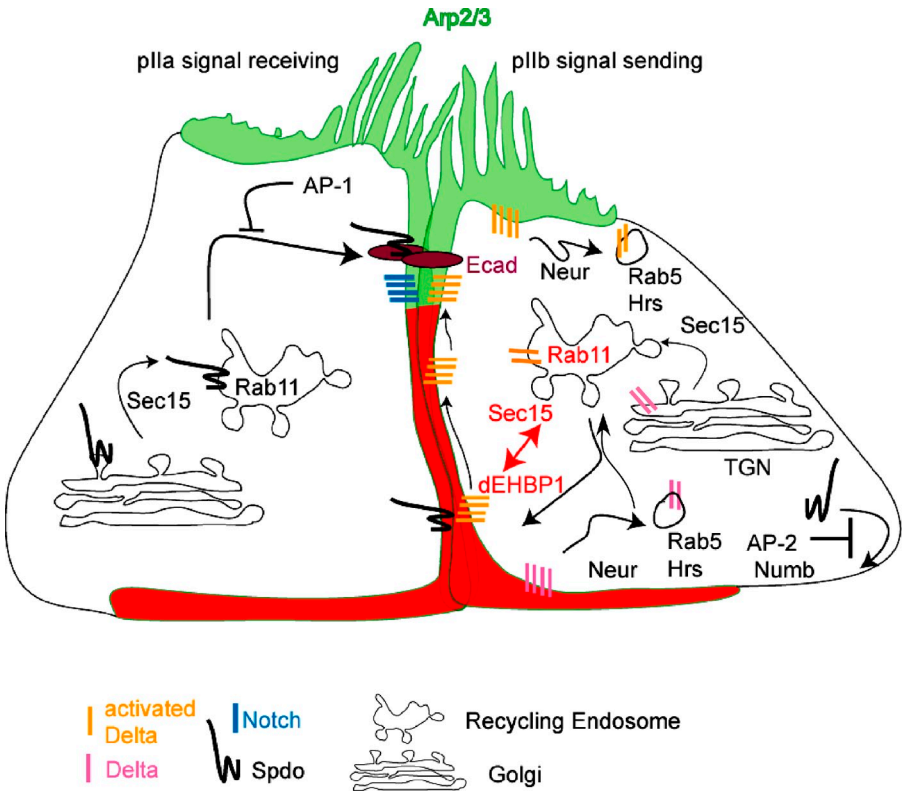

Figure 9. **Model of dEHBP1 function.** Diagram adopted from Rajan et al. (2009), depicting a revised version of Delta recycling pathway. Neur-mediated endocytosis of Delta occurs at both the basal and the apical sides of the pIIb cell and results in the delivery of Delta to Rab5 early endosomes (Benhra et al., 2011). A fraction of Delta then follows a Rab11–Sec15-dependent route (Emery et al., 2005; Jafar-Nejad et al., 2005; Benhra et al., 2011) toward the ARS (Rajan et al., 2009). dEHBP1 (represented by red region overlapping the green region marking the ARS) is enriched at the actin-rich interface of the asymmetrically dividing pII cells where it may facilitate the localization of Delta via its interaction with Sec15 and Rab11. AP-2 and Numb inhibit the localization of Spdo at the plasma membrane of the pIIb cell (O'Connor-Giles and Skeath, 2003; Hutterer and Knoblich, 2005), while AP-1 inhibits the recycling of Spdo toward the apical portion of the pIIa cell (Benhra et al., 2010). Spdo depends on Sec15 activity to reach the plasma membrane (Tong et al., 2010).

Df(2R)ED3181/CyO, ywUbx-FLP; FRT42D UbiGFP, ywUbx-FLP; FRT42D UbiGFP PcDNA, hsFLP tub-GAL4 UAS-GFP;; FRT82B y+ tub-GAL80/TM6, UAS-mCherry-dEHBP1, UAS-Flag-dEHBP1, P{lArB}neurA101 ry506/TM3, ry^{RK} Sb^{1} Ser^{1}, P{GawB}neurGAL4-A101 Kg^{V} /TM3, Sb^{1} (BL #6393), *UAS-cd8GFP, UAS-Rab5-YFP, UAS-Rab7-YFP, UAS-Rab8-YFP, UAS-Rab9-YFP, UAS-Rab10-YFP, UAS-Rab11-YFP, UAS-Sec15-GFP, UAS-Spdo-GFP, FRT82Bsec15^{3}/TM6B, yw;P{tubP-GAL4}LL7/TM3, Sb^{1}*. All crosses were performed on standard media at 25°C unless otherwise indicated. Fly strains bearing the docking sites VK00033 and/or VK00020 were used for injections of the cDNA and genomic rescue constructs, respectively. Fly transformation was mediated by phiC31 transgenesis according to standard protocols.

cDNA and genomic rescue

cDNA constructs were constructed by PCR amplification of *CG15609 isoform B*, *rab11*, and *sec15* with appropriately designed primers and subsequent cloning into suitable vectors. Cloning protocols and DNA purification were performed according to standard protocols. Primer sequences are available upon request.

The genomic rescue construct was constructed by recombineering the 9.1-kb region from gene *CG6805* to gene *CG8963*, residing on either side of *CG15609*, into the F25 P[acman] vector (Venken et al., 2006). All constructs were verified by sequencing before injection or transfection.

Antibody production

The full-length cDNA of dEHBP1-B was cloned in pET28a (EMD) as a NotI PCR fragment. The plasmid was transformed into BL21 Rosetta pLys (EMD). Recombinant protein production was induced by addition of IPTG at a final concentration of 1 mM, in two liters of bacterial culture, previously grown at 37°C, OD_{600} nm = 0.7. Induction of recombinant protein production was performed for 3 h at 37°C. Bacteria were then harvested and used for purification of recombinant dEHBP1 under denaturing conditions using metal affinity chromatography with Ni-NTA His-Bind Resins (EMD), according to the manufacturer's instructions.

Immunohistochemistry, confocal microscopy, live imaging, and image processing

Dissections, stainings, Delta endocytosis, and recycling assays were performed as described previously (Le Borgne and Schweisguth, 2003; Jafar-Nejad et al., 2005; Rajan et al., 2009). In brief, for assaying Notch endocytosis, Delta endocytosis, and Delta recycling, pupal thoracic epithelia were dissected at the selected time points after puparium formation (APF) in Schneider's medium, followed by incubation with the appropriate primary antibody (anti-Notch or anti-Delta). In Notch and Delta endocytosis assays, dissections and subsequent incubations were performed at room temperature (RT). The samples were then washed three times in Schneider's medium and fixed in 4% paraformaldehyde in Schneider's medium for 20 min at RT. After washing with Schneider's medium, thoraxes were permeabilized in 1x PBS, 0.2% Triton X-100 (1x PBT) and incubated with other primary antibodies in 1x PBT, 5% normal goat serum (NGS) at 4°C overnight. The following day, samples were washed three times in 1x PBT for 5 min at RT and incubated with appropriate secondary antibodies. For Delta recycling, thoracic epithelia were dissected in Schneider's medium and then incubated with primary anti-Delta monoclonal antibody in Schneider's medium for 1 h on ice, to label the extracellularly accessible pool of Delta molecules while the same time preventing their endocytosis. After this step of incubation, excess antibody was washed away with Schneider's medium and thoraxes were fixed in 4% paraformaldehyde in Schneider's medium for 20 min at RT either immediately (0-min time point, exocytosed Delta) or after allowing the internalization and trafficking of Delta at RT for 1 h in Schneider's medium (60-min time point, recycled Delta). After washing, samples were permeabilized and incubated with other primary antibodies as already mentioned. For the exocytosis of Delta, thoracic epithelia were dissected in Schneider's medium and immediately fixed with 4% PFA in Schneider's medium. Then, they were incubated with primary anti-Delta monoclonal antibody in Schneider's medium at 4°C overnight, to label all extracellularly accessible Delta. After washing, samples were permeabilized and incubated with other primary antibodies as already mentioned.

Primary antibodies used in this study are: mouse α-Arm 1:100 (N2 7A1, Developmental Studies Hybridoma Bank [DSHB], Iowa City, IA; Peifer et al., 1994), rabbit α-Avl (Lu and Bilder, 2005), rabbit α-Baz 1:1,000 (Wodarz et al., 1999), mouse α-Cut 1:500 (2B10, DSHB; Blochlinger et al., 1990, 1993), mouse α-Delta 1:1,000 (C54.9B, DSHB; Klueg et al., 1998; Qi et al., 1999), mouse α-Dlg 1:100 (4F3, DSHB; Parnas et al., 2001), rat α-E-Cad 1:100 (DCAD2, DSHB; Oda et al., 1994), mouse α-FasIII (7G10, DSHB; Patel et al., 1987), rat α-Elav 1:500 (7E8A10, DSHB), guinea pig α-Hsc3 1:500 (Ryoo et al., 2007), rabbit anti-Hook (Krämer and Phistry, 1996), guinea pig α-HRS 1:600 (Lloyd et al., 2002), rabbit (O'Neill et al., 1994) α-Neur 1:600 (Lai and Rubin, 2001), mouse α-NICD 1:100 (C458.2H, DSHB), rabbit α-Numb 1:1,000 (Rhyu et al., 1994), rabbit α-Patj 1:500 (Bhat et al., 1999), rabbit α-Pros 1:1,000 (Y.N. Jan, HHMI, University of California, San Francisco, San Francisco, CA), mouse anti-Rab1

(Satoh et al., 1997), mouse α-Rab11 antibody 1:200 (BD; Khodosh et al., 2006), guinea pig α-Sec15 1:2,000 (Mehta et al., 2005), guinea pig α-Sens (Nolo et al., 2000), rat α-Spdo 1:200 (O'Connor-Giles and Skeath, 2003), rat α-Su(H) (a kind gift from F. Schweisguth, Institut Pasteur, Paris, France), rat α-Ttk69 1:500 (P. Badenhorst, MRC Laboratory of Molecular Biology, Cambridge, UK; Guo et al., 1995). Alexa 488–conjugated (Invitrogen) and Cy2-, Cy3-, and Cy5-conjugated (Jackson ImmunoResearch Laboratories) secondary antibodies were used at 1:200–1:500.

Live imaging of pupae were performed as described previously (Zitserman and Roegiers, 2011) using an inverted microscope (model TE2000U; Nikon) equipped with a C1 confocal imaging system (488-, 543-, and 633-nm lasers; Nikon) and using a 60x 1.45 NA objective. In brief, pupae at the selected developmental time points were mounted on double-stick tape on a slide dorsal side up. The pupal case was removed carefully so that the thorax and anterior portion of the abdomen were revealed without puncturing them. The pupae were then freed from the pupal case and transferred by a soft brush to be subsequently mounted between a glass slide and coverslip: The pupae were surrounded by a moistened frame of Whatman paper. A continuous bead of silicone vacuum grease extruded from a 5-cc syringe functioned to seal the slide–coverslip combination, protecting the pupa from desiccation and elevating the coverslip so it rested gently on the pupal thorax. A small drop of water (1 µl) at the interface between the coverslip and thorax cuticle was then applied to improve image quality when using immersion objectives. Frames were taken every minute during a time period that initiated at the pI stage, just before cytokinesis, and lasted well into the pII cell stage.

All other confocal scans were acquired with a confocal microscope (model LSM510; Carl Zeiss) with its accompanying software using Plan Apochromat 40× NA 1.4 and Plan Apochromat 63× NA 1.4 objectives (Carl Zeiss). Samples were mounted in Vectashield (Vector Laboratories). Images of fly adult thoraces (treated by boiling in 10% KOH, dissected and mounted in 70% glycerol) were captured with a camera (MicroFire; Olympus) mounted to a stereomicroscope (model MZ16; Leica) using ImagePro Plus 5.0 acquisition software (Media Cybernetics).

Quantification and statistics

Image processing (Z-reslicing and projections) and quantifications were performed using ImageJ software (National Institutes of Health). Fluorescence of Delta was quantified by measuring the mean gray value of pixel intensity in the corresponding channel in XY maximal projections of stacks of confocal sections of ESO lineages and within areas delineated by Sens nuclear staining and expanded by 20% to include Delta punctae toward the periphery of the cells. Stacks were typically spanning the area from apical to basal side of ESO clusters, containing more than 70 optical sections. A similar calculation was performed in areas of same size, but consisting of only epithelial cells and devoid of any ESO clusters, so that the background fluorescence would be estimated and subtracted from the fluorescence intensity value of Delta within the ESO lineages. Images were assembled in Canvas X software (ACDSee Products).

S2 cell culture, transfections, and coimmunoprecipitation

S2 cells were maintained in Schneider's medium, supplemented with 10% heat-inactivated, filter-sterilized fetal bovine serum (FBS) (Sigma-Aldrich) and 1× penicillin and streptomycin antibiotic mix (Invitrogen). Handling of S2 cells was performed according to manufacturer's instructions (Invitrogen).

Transfections of S2 cells were performed using Effectene (QIAGEN) using 0.4 µg of total DNA/1.5 $\times 10^6$ cells according to manufacturer's instructions. For each type of coimmunoprecipitation (coIP), three wells of $\sim 5 \times 10^6$ cells in total were seeded for transfection. Cells were harvested 48 h after transfection, into 15-ml Falcon polypropylene tubes by pipetting. After centrifugation at RT at 1,500 rpm for 5 min, the cells were washed in 1× PBS (equilibrated at RT) and centrifuged as before. The cells were then suspended in 0.2 volumes of ice-cold lysis buffer (50 mM Tris, pH 7.5, 150 mM NaCl, 5% glycerol, and 0.2% Triton X-100), supplemented with EDTA-free cocktail of protease inhibitors (Roche) and placed on ice for 60 min with occasional mild agitation. The lysate was then cleared by centrifugation at 13,000 rpm at 4°C for 10 min. After removing one tenth of the volume for input control, 30 µl of 50% EZ red anti FLAG M2 or EZ red anti-HA Agarose beads slurry (Sigma-Aldrich) was added to each coIP reaction used. The beads had been previously equilibrated in cold lysis buffer including EDTA-free protease inhibitors (Roche). Binding was performed for at least 4 h at 4°C. After centrifugation at 3,000 rpm at 4°C, the supernatant was discarded and the beads were washed with ice-cold lysis buffer, including EDTA-free protease inhibitors. The procedure was repeated two more times. The beads were finally suspended in 1x Laemmli buffer and boiled for 10 min before electrophoresis and Western blot analysis.

GST pull-downs and in vitro translation

pGEX4T-1 and pGEX4T1-Rab11 were transformed into BL21 pLys (Invitrogen) and single colonies were kept as glycerol stocks after being tested for successful induction of corresponding proteins. Overnight cultures were then prepared from the glycerol stocks and used the following morning for inoculation of larger volumes of LB medium at a final dilution of 1:50. The cultures were then allowed to grow at 37°C for ~2 h. GST and GST-Rab11 proteins were induced at 37°C for two additional hours by addition of IPTG at a final concentration of 0.1 mM. Bacteria were lysed in 1x Bugbuster (EMD). Purification of GST proteins from cleared lysates was achieved using GST beads (GE Healthcare) following the manufacturer's instructions. Before binding to in vitro–translated products, beads and proteins were equilibrated in ice-cold lysis buffer containing EDTA-free cocktail of protease inhibitors (Roche), as described above. GST proteins were incubated with in vitro–translated dEHBP1 in ice-cold lysis buffer for at least 5 h at 4°C with rocking.

In vitro translation of *CG15609* isoform B was performed using the TnT T7 Quick Coupled Transcription/Translation System (Promega) combined with the Transcend t-RNA chemiluminescent nonradioactive detection method (Promega). As a template, we used the T7 promoter containing pET28a-dEHBP1 clone, which was originally used for bacterial expression of dEHBP1 in our antibody production experiments.

Online supplemental material

Fig. S1 shows that dEHBP1 does not colocalize with markers of Golgi and early, late, or recycling endosomes (related to Figs. 3 and 4). Fig. S2 shows that the distribution of different subcellular compartments and the integrity of ARS are not affected in the absence of dEHBP1 (related to Fig. 5). Fig. S3 shows that loss of dEHBP1 is epistatic to gain of function of Notch signaling, achieved by ectopic expression of constitutively active $DaPKC^{\Delta N}$ or $Delta^{R+}$, but not by activated $Notch^{NEXT}$. Video 1 shows that mCherry-dEHBP1 is localized within intracellular vesicles and at the interface of pIIa and pIIb cells. Video 2 shows that mCherry-dEHBP1 is localized partially with Spdo-GFP at the apical side of the interface of pIIa and pIIb cells. Video 3 shows that mCherry-dEHBP1 is localized partially with Spdo-GFP at the medial side of the interface of pIIa and pIIb cells. Online supplemental material is available at http://www.jcb.org/cgi/content/full/jcb.201106088/DC1.

We thank the Bloomington Stock Center, and the Developmental Studies Hybridoma Bank for reagents. We are grateful to Dr. Francois Schweisguth for the anti-Su(H), Dr. Marcos Gonzalez-Gaitan for the anti-Rab5 and Dr. Jim Skeath for anti-Spdo antibodies, respectively. The rat α-120kDa antibody was a kind gift from Dr. Satoshi Goto. We thank Yuchun He and Hongling Pan for help with injections. We thank Dr. Manish Jaiswal, Dr. Hamed Jafar-Nejad, Dr. Timothy Mahoney and Dr. Chao Tong and Vafa Bayat for helpful comments on the manuscript.

Confocal microscopy was supported by the National Institutes of Health grant P30HD024064 to the BCM Intellectual and Developmental Disabilities Research Center. N.G. has been supported by European Molecular Biology Organization long term fellowship and Howard Hughes Medical Institute. S.Y. is supported by the Nakajima Foundation. F.R and D.Z. are supported by NIH RO1 NS059971 grant and the Pennsylvania Tobacco Settlement fund. H.B. is an HHMI Investigator.

Submitted: 14 June 2011
Accepted: 29 November 2011

References

Acar, M., H. Jafar-Nejad, H. Takeuchi, A. Rajan, D. Ibrani, N.A. Rana, H. Pan, R.S. Haltiwanger, and H.J. Bellen. 2008. Rumi is a CAP10 domain glycosyltransferase that modifies Notch and is required for Notch signaling. *Cell*. 132:247–258. http://dx.doi.org/10.1016/j.cell.2007.12.016

Andrews, H.K., N. Giagtzoglou, S. Yamamoto, K.L. Schulze, and H.J. Bellen. 2009. Sequoia regulates cell fate decisions in the external sensory organs of adult *Drosophila*. *EMBO Rep.* 10:636–641. http://dx.doi.org/10.1038/embor.2009.66

Ang, A.L., H. Fölsch, U.M. Koivisto, M. Pypaert, and I. Mellman. 2003. The Rab8 GTPase selectively regulates AP-1B-dependent basolateral transport in polarized Madin-Darby canine kidney cells. *J. Cell Biol.* 163:339–350. http://dx.doi.org/10.1083/jcb.200307046

Artavanis-Tsakonas, S., M.D. Rand, and R.J. Lake. 1999. Notch signaling: cell fate control and signal integration in development. *Science*. 284:770–776. http://dx.doi.org/10.1126/science.284.5415.770

Babaoglan, A.B., K.M. O'Connor-Giles, H. Mistry, A. Schickedanz, B.A. Wilson, and J.B. Skeath. 2009. Sanpodo: a context-dependent activator and inhibitor of Notch signaling during asymmetric divisions. *Development*. 136:4089–4098. http://dx.doi.org/10.1242/dev.040386

Banks, S.M., B. Cho, S.H. Eun, J.H. Lee, S.L. Windler, X. Xie, D. Bilder, and J.A. Fischer. 2011. The functions of auxilin and Rab11 in *Drosophila* suggest that the fundamental role of ligand endocytosis in notch signaling cells is not recycling. *PLoS ONE*. 6:e18259. http://dx.doi.org/10.1371/journal.pone.0018259

Bellaïche, Y., and F. Schweisguth. 2001. Lineage diversity in the *Drosophila* nervous system. *Curr. Opin. Genet. Dev.* 11:418–423. http://dx.doi.org/10.1016/S0959-437X(00)00212-4

Benhra, N., F. Vignaux, A. Dussert, F. Schweisguth, and R. Le Borgne. 2010. Neuralized promotes basal to apical transcytosis of delta in epithelial cells. *Mol. Biol. Cell*. 21:2078–2086. http://dx.doi.org/10.1091/mbc.E09-11-0926

Benhra, N., S. Lallet, M. Cotton, S. Le Bras, A. Dussert, and R. Le Borgne. 2011. AP-1 controls the trafficking of Notch and Sanpodo toward E-cadherin junctions in sensory organ precursors. *Curr. Biol.* 21:87–95. http://dx.doi.org/10.1016/j.cub.2010.12.010

Berdnik, D., T. Török, M. González-Gaitán, and J.A. Knoblich. 2002. The endocytic protein alpha-Adaptin is required for numb-mediated asymmetric cell division in *Drosophila*. *Dev. Cell*. 3:221–231. http://dx.doi.org/10.1016/S1534-5807(02)00215-0

Betschinger, J., K. Mechtler, and J.A. Knoblich. 2003. The Par complex directs asymmetric cell division by phosphorylating the cytoskeletal protein Lgl. *Nature*. 422:326–330. http://dx.doi.org/10.1038/nature01486

Bhat, M.A., S. Izaddoost, Y. Lu, K.O. Cho, K.W. Choi, and H.J. Bellen. 1999. Discs Lost, a novel multi-PDZ domain protein, establishes and maintains epithelial polarity. *Cell*. 96:833–845. http://dx.doi.org/10.1016/S0092-8674(00)80593-0

Blochlinger, K., R. Bodmer, L.Y. Jan, and Y.N. Jan. 1990. Patterns of expression of cut, a protein required for external sensory organ development in wild-type and cut mutant *Drosophila* embryos. *Genes Dev.* 4:1322–1331. http://dx.doi.org/10.1101/gad.4.8.1322

Blochlinger, K., L.Y. Jan, and Y.N. Jan. 1993. Postembryonic patterns of expression of cut, a locus regulating sensory organ identity in *Drosophila*. *Development*. 117:441–450.

Bolós, V., M. Blanco, V. Medina, G. Aparicio, S. Díaz-Prado, and E. Grande. 2009. Notch signalling in cancer stem cells. *Clin. Transl. Oncol.* 11:11–19. http://dx.doi.org/10.1007/s12094-009-0305-2

Bray, S.J. 2006. Notch signalling: a simple pathway becomes complex. *Nat. Rev. Mol. Cell Biol.* 7:678–689. http://dx.doi.org/10.1038/nrm2009

Cook, K.R., A.L. Parks, L.M. Jacobus, T.C. Kaufman, and K.A. Matthews. 2010. New research resources at the Bloomington *Drosophila* Stock Center. *Fly (Austin)*. 4:88–91. http://dx.doi.org/10.4161/fly.4.1.11230

Cotta-de-Almeida, V., L. Westerberg, M.H. Maillard, D. Onaldi, H. Wachtel, P. Meelu, U.I. Chung, R. Xavier, F.W. Alt, and S.B. Snapper. 2007. Wiskott Aldrich syndrome protein (WASP) and N-WASP are critical for T cell development. *Proc. Natl. Acad. Sci. USA*. 104:15424–15429. http://dx.doi.org/10.1073/pnas.0706881104

Coumailleau, F., M. Fürthauer, J.A. Knoblich, and M. González-Gaitán. 2009. Directional Delta and Notch trafficking in Sara endosomes during asymmetric cell division. *Nature*. 458:1051–1055. http://dx.doi.org/10.1038/nature07854

Das, A., and W. Guo. 2011. Rabs and the exocyst in ciliogenesis, tubulogenesis and beyond. *Trends Cell Biol.* 21:383–386. http://dx.doi.org/10.1016/j.tcb.2011.03.006

Dye, C.A., J.K. Lee, R.C. Atkinson, R. Brewster, P.L. Han, and H.J. Bellen. 1998. The *Drosophila* sanpodo gene controls sibling cell fate and encodes a tropomodulin homolog, an actin/tropomyosin-associated protein. *Development*. 125:1845–1856.

Emery, G., A. Hutterer, D. Berdnik, B. Mayer, F. Wirtz-Peitz, M.G. Gaitan, and J.A. Knoblich. 2005. Asymmetric Rab 11 endosomes regulate delta recycling and specify cell fate in the *Drosophila* nervous system. *Cell*. 122:763–773. http://dx.doi.org/10.1016/j.cell.2005.08.017

Fortini, M.E. 2009. Notch signaling: the core pathway and its posttranslational regulation. *Dev. Cell*. 16:633–647. http://dx.doi.org/10.1016/j.devcel.2009.03.010

Fortini, M.E., and D. Bilder. 2009. Endocytic regulation of Notch signaling. *Curr. Opin. Genet. Dev.* 19:323–328. http://dx.doi.org/10.1016/j.gde.2009.04.005

Friedberg, F. 2010. Singlet CH domain containing human multidomain proteins: an inventory. *Mol. Biol. Rep.* 37:1531–1539. http://dx.doi.org/10.1007/s11033-009-9554-y

Fürthauer, M., and M. González-Gaitán. 2009a. Endocytic regulation of notch signalling during development. *Traffic*. 10:792–802. http://dx.doi.org/10.1111/j.1600-0854.2009.00914.x

Fürthauer, M., and M. González-Gaitán. 2009b. Endocytosis, asymmetric cell division, stem cells and cancer: unus pro omnibus, omnes pro uno. *Mol. Oncol.* 3:339–353. http://dx.doi.org/10.1016/j.molonc.2009.05.006

Gallagher, C.M., and J.A. Knoblich. 2006. The conserved c2 domain protein lethal (2) giant discs regulates protein trafficking in *Drosophila*. *Dev. Cell*. 11:641–653. http://dx.doi.org/10.1016/j.devcel.2006.09.014

Gho, M., Y. Bellaïche, and F. Schweisguth. 1999. Revisiting the *Drosophila* microchaete lineage: a novel intrinsically asymmetric cell division generates a glial cell. *Development*. 126:3573–3584.

Gimona, M., and R. Mital. 1998. The single CH domain of calponin is neither sufficient nor necessary for F-actin binding. *J. Cell Sci.* 111:1813–1821.

Gimona, M., K. Djinovic-Carugo, W.J. Kranewitter, and S.J. Winder. 2002. Functional plasticity of CH domains. *FEBS Lett.* 513:98–106. http://dx.doi.org/10.1016/S0014-5793(01)03240-9

Gönczy, P. 2008. Mechanisms of asymmetric cell division: flies and worms pave the way. *Nat. Rev. Mol. Cell Biol.* 9:355–366. http://dx.doi.org/10.1038/nrm2388

Gridley, T. 2003. Notch signaling and inherited disease syndromes. *Hum. Mol. Genet.* 12(Spec No 1):R9–R13. http://dx.doi.org/10.1093/hmg/ddg052

Gridley, T. 2007. Notch signaling in vascular development and physiology. *Development*. 134:2709–2718. http://dx.doi.org/10.1242/dev.004184

Guichard, A., S.M. McGillivray, B. Cruz-Moreno, N.M. van Sorge, V. Nizet, and E. Bier. 2010. Anthrax toxins cooperatively inhibit endocytic recycling by the Rab11/Sec15 exocyst. *Nature*. 467:854–858. http://dx.doi.org/10.1038/nature09446

Guilherme, A., N.A. Soriano, S. Bose, J. Holik, A. Bose, D.P. Pomerleau, P. Furcinitti, J. Leszyk, S. Corvera, and M.P. Czech. 2004a. EHD2 and the novel EH domain binding protein EHBP1 couple endocytosis to the actin cytoskeleton. *J. Biol. Chem.* 279:10593–10605. http://dx.doi.org/10.1074/jbc.M307702200

Guilherme, A., N.A. Soriano, P.S. Furcinitti, and M.P. Czech. 2004b. Role of EHD1 and EHBP1 in perinuclear sorting and insulin-regulated GLUT4 recycling in 3T3-L1 adipocytes. *J. Biol. Chem.* 279:40062–40075. http://dx.doi.org/10.1074/jbc.M401918200

Guo, M., E. Bier, L.Y. Jan, and Y.N. Jan. 1995. tramtrack acts downstream of numb to specify distinct daughter cell fates during asymmetric cell divisions in the *Drosophila* PNS. *Neuron*. 14:913–925. http://dx.doi.org/10.1016/0896-6273(95)90330-5

Henry, L., and D.R. Sheff. 2008. Rab8 regulates basolateral secretory, but not recycling, traffic at the recycling endosome. *Mol. Biol. Cell*. 19:2059–2068. http://dx.doi.org/10.1091/mbc.E07-09-0902

Huber, L.A., S. Pimplikar, R.G. Parton, H. Virta, M. Zerial, and K. Simons. 1993. Rab8, a small GTPase involved in vesicular traffic between the TGN and the basolateral plasma membrane. *J. Cell Biol.* 123:35–45. http://dx.doi.org/10.1083/jcb.123.1.35

Humbert, P., S. Russell, and H. Richardson. 2003. Dlg, Scribble and Lgl in cell polarity, cell proliferation and cancer. *Bioessays*. 25:542–553. http://dx.doi.org/10.1002/bies.10286

Hutterer, A., and J.A. Knoblich. 2005. Numb and alpha-Adaptin regulate Sanpodo endocytosis to specify cell fate in *Drosophila* external sensory organs. *EMBO Rep.* 6:836–842. http://dx.doi.org/10.1038/sj.embor.7400500

Jafar-Nejad, H., H.K. Andrews, M. Acar, V. Bayat, F. Wirtz-Peitz, S.Q. Mehta, J.A. Knoblich, and H.J. Bellen. 2005. Sec15, a component of the exocyst, promotes notch signaling during the asymmetric division of *Drosophila* sensory organ precursors. *Dev. Cell*. 9:351–363. http://dx.doi.org/10.1016/j.devcel.2005.06.010

Kaun, K.R., R. Azanchi, Z. Maung, J. Hirsh, and U. Heberlein. 2011. A *Drosophila* model for alcohol reward. *Nat. Neurosci.* 14:612–619. http://dx.doi.org/10.1038/nn.2805

Khodosh, R., A. Augsburger, T.L. Schwarz, and P.A. Garrity. 2006. Bchs, a BEACH domain protein, antagonizes Rab11 in synapse morphogenesis and other developmental events. *Development*. 133:4655–4665. http://dx.doi.org/10.1242/dev.02650

Klueg, K.M., T.R. Parody, and M.A. Muskavitch. 1998. Complex proteolytic processing acts on Delta, a transmembrane ligand for Notch, during *Drosophila* development. *Mol. Biol. Cell*. 9:1709–1723.

Kopan, R., and M.X. Ilagan. 2009. The canonical Notch signaling pathway: unfolding the activation mechanism. *Cell*. 137:216–233. http://dx.doi.org/10.1016/j.cell.2009.03.045

Korenbaum, E., and F. Rivero. 2002. Calponin homology domains at a glance. *J. Cell Sci.* 115:3543–3545. http://dx.doi.org/10.1242/jcs.00003

Krämer, H., and M. Phistry. 1996. Mutations in the *Drosophila* hook gene inhibit endocytosis of the boss transmembrane ligand into multivesicular bodies. *J. Cell Biol.* 133:1205–1215. http://dx.doi.org/10.1083/jcb.133.6.1205

Lai, E.C. 2004. Notch signaling: control of cell communication and cell fate. *Development*. 131:965–973. http://dx.doi.org/10.1242/dev.01074

Lai, E.C., and V. Orgogozo. 2004. A hidden program in *Drosophila* peripheral neurogenesis revealed: fundamental principles underlying sensory organ diversity. *Dev. Biol*. 269:1–17. http://dx.doi.org/10.1016/j.ydbio.2004.01.032

Lai, E.C., and G.M. Rubin. 2001. *neuralized* functions cell-autonomously to regulate a subset of notch-dependent processes during adult *Drosophila* development. *Dev. Biol.* 231:217–233. http://dx.doi.org/10.1006/dbio.2000.0124

Langevin, J., R. Le Borgne, F. Rosenfeld, M. Gho, F. Schweisguth, and Y. Bellaïche. 2005. Lethal giant larvae controls the localization of notch-signaling regulators numb, neuralized, and Sanpodo in *Drosophila* sensory-organ precursor cells. *Curr. Biol.* 15:955–962. http://dx.doi.org/10.1016/j.cub.2005.04.054

Le Borgne, R., and F. Schweisguth. 2003. Unequal segregation of Neuralized biases Notch activation during asymmetric cell division. *Dev. Cell*. 5:139–148. http://dx.doi.org/10.1016/S1534-5807(03)00187-4

Le Borgne, R., A. Bardin, and F. Schweisguth. 2005. The roles of receptor and ligand endocytosis in regulating Notch signaling. *Development*. 132:1751–1762. http://dx.doi.org/10.1242/dev.01789

Lloyd, T.E., R. Atkinson, M.N. Wu, Y. Zhou, G. Pennetta, and H.J. Bellen. 2002. Hrs regulates endosome membrane invagination and tyrosine kinase receptor signaling in *Drosophila*. *Cell*. 108:261–269. http://dx.doi.org/10.1016/S0092-8674(02)00611-6

Lu, H., and D. Bilder. 2005. Endocytic control of epithelial polarity and proliferation in *Drosophila*. *Nat. Cell Biol.* 7:1232–1239. http://dx.doi.org/10.1038/ncb1324

Mehta, S.Q., P.R. Hiesinger, S. Beronja, R.G. Zhai, K.L. Schulze, P. Verstreken, Y. Cao, Y. Zhou, U. Tepass, M.C. Crair, and H.J. Bellen. 2005. Mutations in *Drosophila* sec15 reveal a function in neuronal targeting for a subset of exocyst components. *Neuron*. 46:219–232. http://dx.doi.org/10.1016/j.neuron.2005.02.029

Nichols, J.T., A. Miyamoto, S.L. Olsen, B. D'Souza, C. Yao, and G. Weinmaster. 2007a. DSL ligand endocytosis physically dissociates Notch1 heterodimers before activating proteolysis can occur. *J. Cell Biol.* 176:445–458. http://dx.doi.org/10.1083/jcb.200609014

Nichols, J.T., A. Miyamoto, and G. Weinmaster. 2007b. Notch signaling—constantly on the move. *Traffic*. 8:959–969. http://dx.doi.org/10.1111/j.1600-0854.2007.00592.x

Nolo, R., L.A. Abbott, and H.J. Bellen. 2000. Senseless, a Zn finger transcription factor, is necessary and sufficient for sensory organ development in *Drosophila*. *Cell*. 102:349–362. http://dx.doi.org/10.1016/S0092-8674(00)00040-4

O'Connor-Giles, K.M., and J.B. Skeath. 2003. Numb inhibits membrane localization of Sanpodo, a four-pass transmembrane protein, to promote asymmetric divisions in *Drosophila*. *Dev. Cell*. 5:231–243. http://dx.doi.org/10.1016/S1534-5807(03)00226-0

O'Neill, E.M., I. Rebay, R. Tjian, and G.M. Rubin. 1994. The activities of two Ets-related transcription factors required for *Drosophila* eye development are modulated by the Ras/MAPK pathway. *Cell*. 78:137–147. http://dx.doi.org/10.1016/0092-8674(94)90580-0

Oda, H., T. Uemura, Y. Harada, Y. Iwai, and M. Takeichi. 1994. A *Drosophila* homolog of cadherin associated with armadillo and essential for embryonic cell-cell adhesion. *Dev. Biol.* 165:716–726. http://dx.doi.org/10.1006/dbio.1994.1287

Okabe, M., T. Imai, M. Kurusu, Y. Hiromi, and H. Okano. 2001. Translational repression determines a neuronal potential in *Drosophila* asymmetric cell division. *Nature*. 411:94–98. http://dx.doi.org/10.1038/35075094

Parks, A.L., K.M. Klueg, J.R. Stout, and M.A. Muskavitch. 2000. Ligand endocytosis drives receptor dissociation and activation in the Notch pathway. *Development*. 127:1373–1385.

Parks, A.L., K.R. Cook, M. Belvin, N.A. Dompe, R. Fawcett, K. Huppert, L.R. Tan, C.G. Winter, K.P. Bogart, J.E. Deal, et al. 2004. Systematic generation of high-resolution deletion coverage of the *Drosophila melanogaster* genome. *Nat. Genet.* 36:288–292. http://dx.doi.org/10.1038/ng1312

Parnas, D., A.P. Haghighi, R.D. Fetter, S.W. Kim, and C.S. Goodman. 2001. Regulation of postsynaptic structure and protein localization by the Rho-type guanine nucleotide exchange factor dPix. *Neuron*. 32:415–424. http://dx.doi.org/10.1016/S0896-6273(01)00485-8

Patel, N.H., P.M. Snow, and C.S. Goodman. 1987. Characterization and cloning of fasciclin III: a glycoprotein expressed on a subset of neurons and axon pathways in *Drosophila*. *Cell*. 48:975–988. http://dx.doi.org/10.1016/0092-8674(87)90706-9

Pavlopoulos, E., C. Pitsouli, K.M. Klueg, M.A. Muskavitch, N.K. Moschonas, and C. Delidakis. 2001. *neuralized* Encodes a peripheral membrane protein involved in delta signaling and endocytosis. *Dev. Cell*. 1:807–816. http://dx.doi.org/10.1016/S1534-5807(01)00093-4

Peifer, M., D. Sweeton, M. Casey, and E. Wieschaus. 1994. *wingless* signal and Zeste-white 3 kinase trigger opposing changes in the intracellular distribution of Armadillo. *Development*. 120:369–380.

Pereira-Leal, J.B., and M.C. Seabra. 2001. Evolution of the Rab family of small GTP-binding proteins. *J. Mol. Biol.* 313:889–901. http://dx.doi.org/10.1006/jmbi.2001.5072

Pi, H., H.J. Wu, and C.T. Chien. 2001. A dual function of phyllopod in *Drosophila* external sensory organ development: cell fate specification of sensory organ precursor and its progeny. *Development*. 128:2699–2710.

Qi, H., M.D. Rand, X. Wu, N. Sestan, W. Wang, P. Rakic, T. Xu, and S. Artavanis-Tsakonas. 1999. Processing of the notch ligand delta by the metalloprotease Kuzbanian. *Science*. 283:91–94. http://dx.doi.org/10.1126/science.283.5398.91

Radtke, F., N. Fasnacht, and H.R. Macdonald. 2010. Notch signaling in the immune system. *Immunity*. 32:14–27. http://dx.doi.org/10.1016/j.immuni.2010.01.004

Rajan, A., A.C. Tien, C.M. Haueter, K.L. Schulze, and H.J. Bellen. 2009. The Arp2/3 complex and WASp are required for apical trafficking of Delta into microvilli during cell fate specification of sensory organ precursors. *Nat. Cell Biol.* 11:815–824. http://dx.doi.org/10.1038/ncb1888

Reddy, G.V., and V. Rodrigues. 1999. A glial cell arises from an additional division within the mechanosensory lineage during development of the microchaete on the *Drosophila* notum. *Development*. 126:4617–4622.

Rhyu, M.S., L.Y. Jan, and Y.N. Jan. 1994. Asymmetric distribution of numb protein during division of the sensory organ precursor cell confers distinct fates to daughter cells. *Cell*. 76:477–491. http://dx.doi.org/10.1016/0092-8674(94)90112-0

Roegiers, F., L.Y. Jan, and Y.N. Jan. 2005. Regulation of membrane localization of Sanpodo by lethal giant larvae and neuralized in asymmetrically dividing cells of *Drosophila* sensory organs. *Mol. Biol. Cell*. 16:3480–3487. http://dx.doi.org/10.1091/mbc.E05-03-0177

Roy, M., W.S. Pear, and J.C. Aster. 2007. The multifaceted role of Notch in cancer. *Curr. Opin. Genet. Dev*. 17:52–59. http://dx.doi.org/10.1016/j.gde.2006.12.001

Ryder, E., M. Ashburner, R. Bautista-Llacer, J. Drummond, J. Webster, G. Johnson, T. Morley, Y.S. Chan, F. Blows, D. Coulson, et al. 2007. The DrosDel deletion collection: a *Drosophila* genomewide chromosomal deficiency resource. *Genetics*. 177:615–629. http://dx.doi.org/10.1534/genetics.107.076216

Ryoo, H.D., P.M. Domingos, M.J. Kang, and H. Steller. 2007. Unfolded protein response in a *Drosophila* model for retinal degeneration. *EMBO J.* 26:242–252. http://dx.doi.org/10.1038/sj.emboj.7601477

Saj, A., Z. Arziman, D. Stempfle, W. van Belle, U. Sauder, T. Horn, M. Dürrenberger, R. Paro, M. Boutros, and G. Merdes. 2010. A combined ex vivo and in vivo RNAi screen for notch regulators in *Drosophila* reveals an extensive notch interaction network. *Dev. Cell*. 18:862–876. http://dx.doi.org/10.1016/j.devcel.2010.03.013

Sasamura, T., N. Sasaki, F. Miyashita, S. Nakao, H.O. Ishikawa, M. Ito, M. Kitagawa, K. Harigaya, E. Spana, D. Bilder, et al. 2003. *neurotic*, a novel maternal neurogenic gene, encodes an *O*-fucosyltransferase that is essential for Notch-Delta interactions. *Development*. 130:4785–4795. http://dx.doi.org/10.1242/dev.00679

Satoh, A., F. Tokunaga, S. Kawamura, and K. Ozaki. 1997. In situ inhibition of vesicle transport and protein processing in the dominant negative Rab1 mutant of *Drosophila*. *J. Cell Sci.* 110:2943–2953.

Seugnet, L., Y. Suzuki, G. Merlin, L. Gottschalk, S.P. Duntley, and P.J. Shaw. 2011. Notch signaling modulates sleep homeostasis and learning after sleep deprivation in *Drosophila*. *Curr. Biol.* 21:835–840. http://dx.doi.org/10.1016/j.cub.2011.04.001

Shi, A., C.C. Chen, R. Banerjee, D. Glodowski, A. Audhya, C. Rongo, and B.D. Grant. 2010. EHBP-1 functions with RAB-10 during endocytic recycling in *Caenorhabditis elegans*. *Mol. Biol. Cell*. 21:2930–2943. http://dx.doi.org/10.1091/mbc.E10-02-0149

Spradling, A.C., D. Stern, A. Beaton, E.J. Rhem, T. Laverty, N. Mozden, S. Misra, and G.M. Rubin. 1999. The Berkeley Drosophila Genome Project gene disruption project: Single *P*-element insertions mutating 25% of vital *Drosophila* genes. *Genetics*. 153:135–177.

Stenmark, H. 2009. Rab GTPases as coordinators of vesicle traffic. *Nat. Rev. Mol. Cell Biol.* 10:513–525. http://dx.doi.org/10.1038/nrm2728

Thrasher, A.J., and S.O. Burns. 2010. WASP: a key immunological multitasker. *Nat. Rev. Immunol.* 10:182–192. http://dx.doi.org/10.1038/nri2724

Tien, A.C., A. Rajan, K.L. Schulze, H.D. Ryoo, M. Acar, H. Steller, and H.J. Bellen. 2008. Ero1L, a thiol oxidase, is required for Notch signaling through cysteine bridge formation of the Lin12-Notch repeats in *Drosophila melanogaster*. *J. Cell Biol.* 182:1113–1125. http://dx.doi.org/10.1083/jcb.200805001

Tien, A.C., A. Rajan, and H.J. Bellen. 2009. A Notch updated. *J. Cell Biol.* 184:621–629. http://dx.doi.org/10.1083/jcb.200811141

Tong, X., D. Zitserman, I. Serebriiskii, M. Andrake, R. Dunbrack, and F. Roegiers. 2010. Numb independently antagonizes Sanpodo membrane targeting and Notch signaling in *Drosophila* sensory organ precursor cells. *Mol. Biol. Cell*. 21:802–810. http://dx.doi.org/10.1091/mbc.E09-09-0831

Vaccari, T., and D. Bilder. 2005. The *Drosophila* tumor suppressor vps25 prevents nonautonomous overproliferation by regulating notch trafficking. *Dev. Cell*. 9:687–698. http://dx.doi.org/10.1016/j.devcel.2005.09.019

Vaccari, T., S. Duchi, K. Cortese, C. Tacchetti, and D. Bilder. 2010. The vacuolar ATPase is required for physiological as well as pathological activation of the Notch receptor. *Development*. 137:1825–1832. http://dx.doi.org/10.1242/dev.045484

Venken, K.J., Y. He, R.A. Hoskins, and H.J. Bellen. 2006. P[acman]: a BAC transgenic platform for targeted insertion of large DNA fragments in *D. melanogaster*. *Science*. 314:1747–1751. http://dx.doi.org/10.1126/science.1134426

Wang, W., and G. Struhl. 2004. *Drosophila* Epsin mediates a select endocytic pathway that DSL ligands must enter to activate Notch. *Development*. 131:5367–5380. http://dx.doi.org/10.1242/dev.01413

Watt, F.M., S. Estrach, and C.A. Ambler. 2008. Epidermal Notch signalling: differentiation, cancer and adhesion. *Curr. Opin. Cell Biol.* 20:171–179. http://dx.doi.org/10.1016/j.ceb.2008.01.010

Weng, A.P., and J.C. Aster. 2004. Multiple niches for Notch in cancer: context is everything. *Curr. Opin. Genet. Dev.* 14:48–54. http://dx.doi.org/10.1016/j.gde.2003.11.004

Windler, S.L., and D. Bilder. 2010. Endocytic internalization routes required for delta/notch signaling. *Curr. Biol.* 20:538–543. http://dx.doi.org/10.1016/j.cub.2010.01.049

Wirtz-Peitz, F., T. Nishimura, and J.A. Knoblich. 2008. Linking cell cycle to asymmetric division: Aurora-A phosphorylates the Par complex to regulate Numb localization. *Cell*. 135:161–173. http://dx.doi.org/10.1016/j.cell.2008.07.049

Wodarz, A., A. Ramrath, U. Kuchinke, and E. Knust. 1999. Bazooka provides an apical cue for Inscuteable localization in *Drosophila* neuroblasts. *Nature*. 402:544–547. http://dx.doi.org/10.1038/990128

Yamamoto, S., W.L. Charng, and H.J. Bellen. 2010. Endocytosis and intracellular trafficking of Notch and its ligands. *Curr. Top. Dev. Biol.* 92:165–200. http://dx.doi.org/10.1016/S0070-2153(10)92005-X

Zhai, R.G., P.R. Hiesinger, T.W. Koh, P. Verstreken, K.L. Schulze, Y. Cao, H. Jafar-Nejad, K.K. Norga, H. Pan, V. Bayat, et al. 2003. Mapping *Drosophila* mutations with molecularly defined P element insertions. *Proc. Natl. Acad. Sci. USA*. 100:10860–10865. http://dx.doi.org/10.1073/pnas.1832753100

Zhang, D., and L. Aravind. 2010. Identification of novel families and classification of the C2 domain superfamily elucidate the origin and evolution of membrane targeting activities in eukaryotes. *Gene*. 469:18–30. http://dx.doi.org/10.1016/j.gene.2010.08.006

Zhang, X.M., S. Ellis, A. Sriratana, C.A. Mitchell, and T. Rowe. 2004. Sec15 is an effector for the Rab11 GTPase in mammalian cells. *J. Biol. Chem.* 279:43027–43034. http://dx.doi.org/10.1074/jbc.M402264200

Zitserman, D., and F. Roegiers. 2011. Live-cell imaging of sensory organ precursor cells in intact *Drosophila* pupae. *J. Vis. Exp.* (51):2706. http://dx.doi.org/10.3791/2706

Giagtzoglou et al., http://www.jcb.org/cgi/content/full/jcb.201106088/DC1

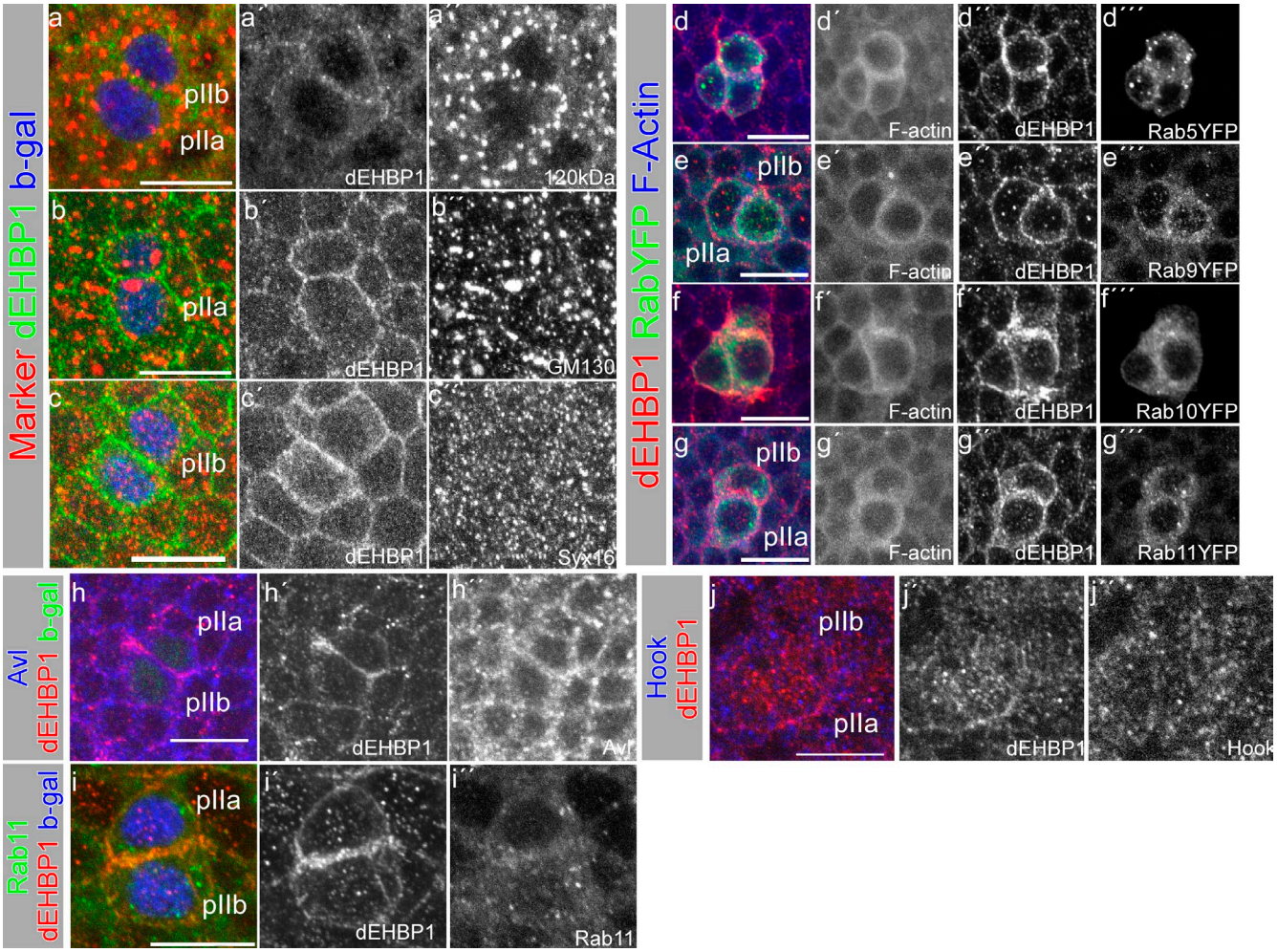

Figure S1. **dEHBP1 does not colocalize with markers of Golgi and early, late, or recycling endosomes (related to Figs. 3 and 4).** (a–c′′) dEHBP1 (a′, b′, and c′) does not colocalize with Golgi markers, p120kD (a′′), GM130 (b′′), or Syx16 (c′′). d-g′′′) dEHBP1 (d′′, e′′, f′′, and g′′) colocalizes with F-actin (d′, e′, f′, and g′) at the interphase of pIIb/pIIa cells (e and g), but it does not colocalize with Rab5YFP (d′′′), Rab9YFP (e′′′), Rab10YFP (f′′′), or Rab11YFP (g′′′), overexpressed in ESO lineages by *neur*^{Gal4}. (h–j′′) dEHBP1 (h′, i′, and j′) does not colocalize with Avl (h′′), Rab11 (i′′), and Hook (j′′), markers of early, recycling, and late endosomes, respectively. Bars, 10 µm.

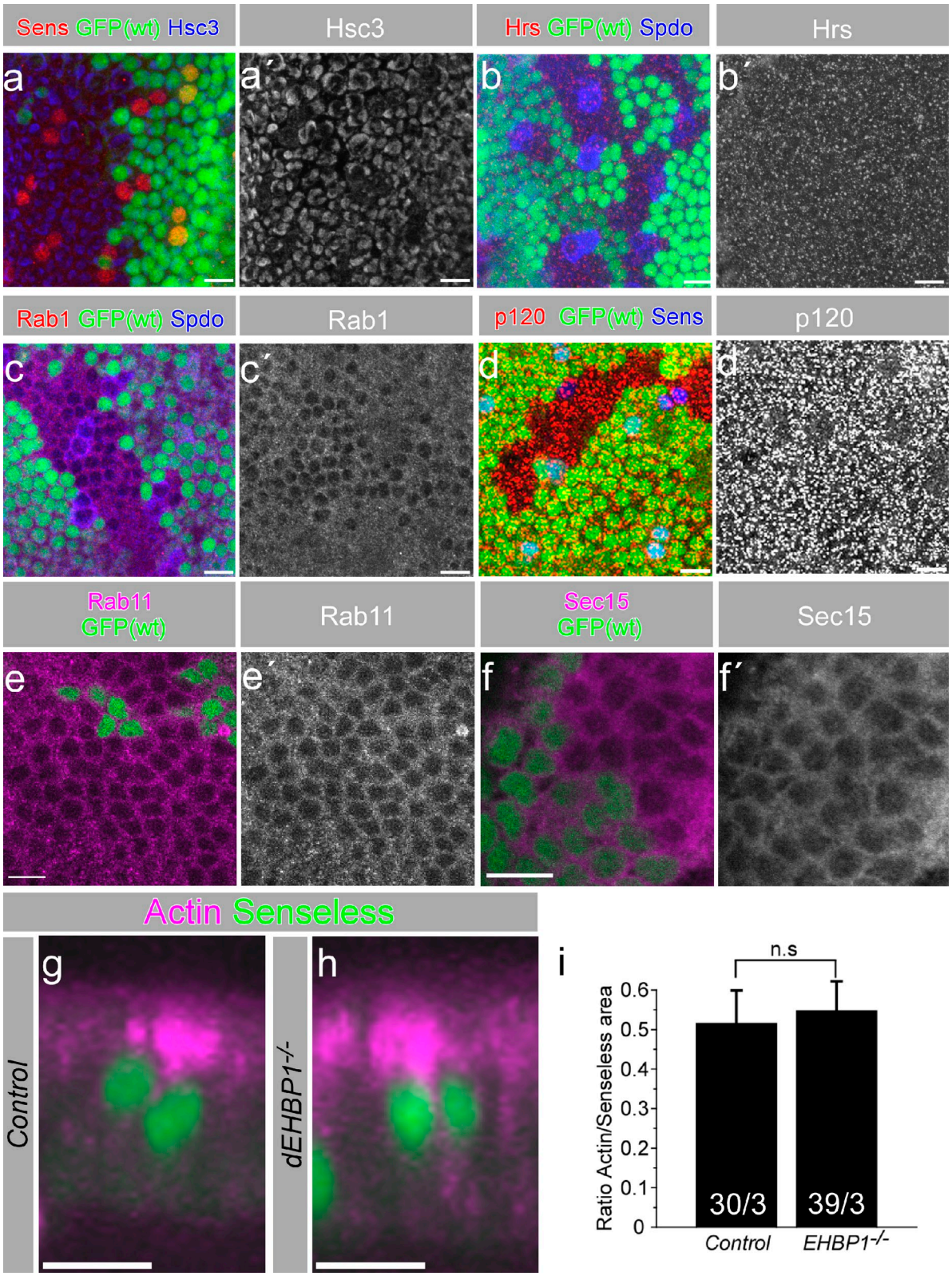

Figure S2. **The distribution of different subcellular compartments and the integrity of ARS are not affected in the absence of dEHBP1 (related to Fig. 5, a-f').** The endoplasmic reticulum marker Hsc3 (a–a'), the late endosomal marker Hrs (b–b'), the Golgi markers Rab1 (c–c') and p120 kD (d–d'), the recycling endosomal marker Rab11 (e–e'), and the exocyst member Sec15 (f–f') are unaffected in the absence of *dEHBP1*. Single channel representations for Hsc3, Hrs, Rab1, p120 kD, Rab11, and Sec15 are shown in a', b', c', d', e', and f', respectively. GFP marks the wild-type region in a, b, c, d, e, and f. (g and h) The characteristic ARS is formed properly between pII cells in the presence (g) or absence of *dEHBP1* (h). Bars (a–h): 10 µm. (i) Quantification of the ratio of the area of Actin to the area of Sens nuclei in the control and *dEHBP1*$^{-/-}$ ESO clusters. Numbers at the base of the bars represent the number of ESO clusters/thoraces used for quantification.

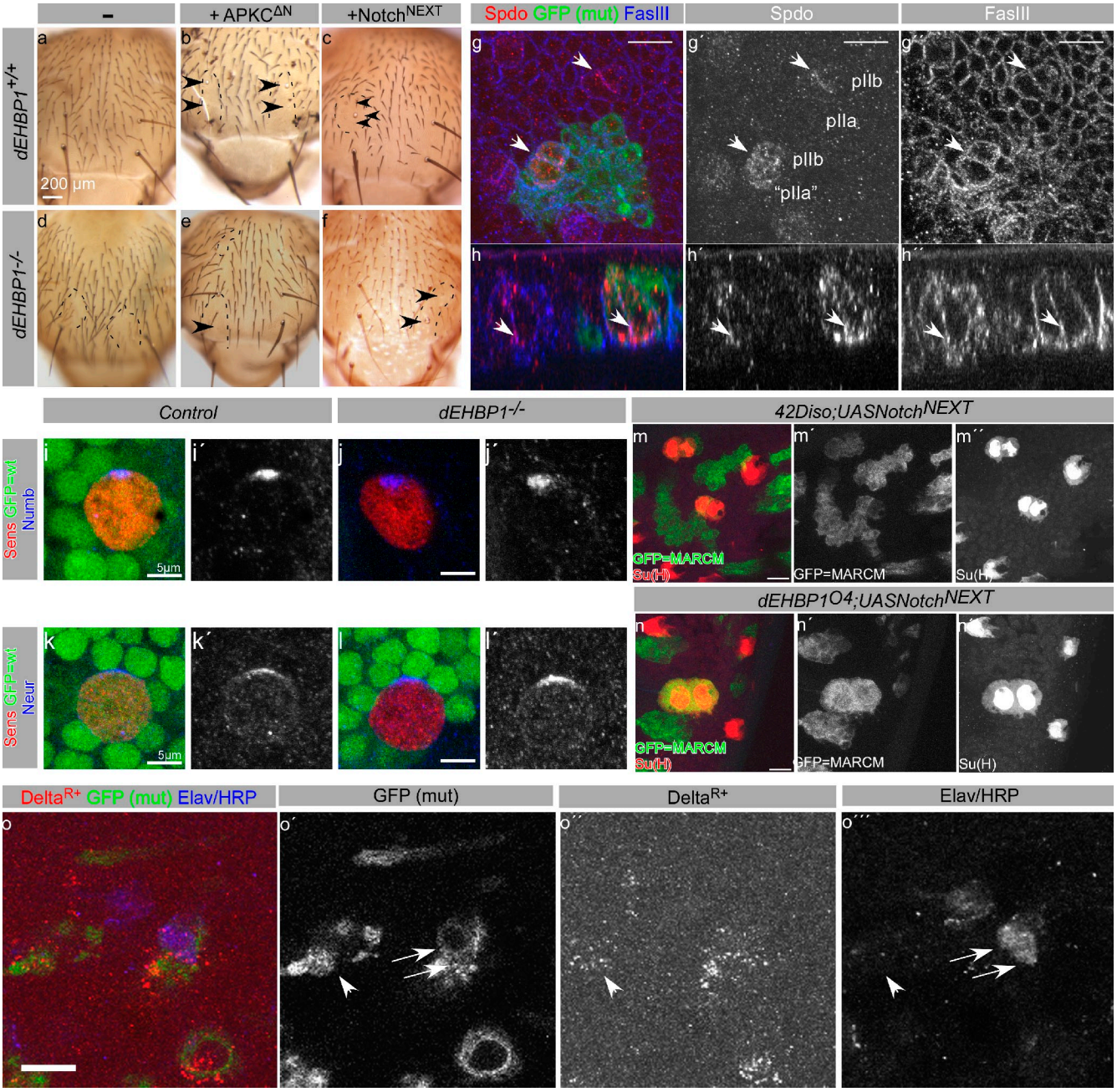

Figure S3. **Loss of dEHBP1 is epistatic to gain of function of Notch signaling, achieved by ectopic expression of constitutively active DaPKC$^{\Delta N}$ or Delta^{R+}, but not by activated Notch^{NEXT}.** (a and b) Loss of *dEHBP1* within thoracic clones results in bald patches of cuticle, devoid of mechanosensory bristles, as outlined by dashed line in b (compare a with b; also see Fig. 1). (b and c) Overexpression of *DaPKC$^{\Delta N}$* (b) or *Notch^{NEXT}* (c) in wild-type (*FRT42Diso*) clones within thoracic epithelia, outlined by dashed line, results in enlarged socket structures, indicated by the arrowheads. (e) Overexpression of *DaPKC$^{\Delta N}$* in the absence of *dEHBP1* within thoracic clones, outlined by dashed line, results in bald patches of cuticle, devoid of mechanosensory bristles, as indicated by the arrowheads. (f) Overexpression of *Notch^{NEXT}* in the absence of *dEHBP1* within thoracic clones, outlined by dashed line, still results in enlarged socket structures, indicated by the arrowheads. (g–h′′) XY sections (g–g′′) and a single XZ section (h–h′′) of thoracic epithelia bearing clones of *dEHBP1^{O4}* overexpressing *DaPKC$^{\Delta N}$*. Please note that Spdo is enriched in the absence of *dEHBP1* (bottom cluster in g′–g′′, right cluster in h′–h′′). Spdo (g′–h′) localizes at the interphase of pII cells, along with the lateral membrane marker FasIII (g′′–h′′), in the presence or absence of dEHBP1, as the arrows indicate. Bars, 10 µm. (i–l′) The localization of the cell fate determinants Numb (i–j′′) and Neur (k–l′′) in the presence (i–i′, k–k′) or absence (j–j′, l–l′) of dEHBP1. Single channel representations for Numb (i′–j′) and Neur (k′–l′) are shown in black and white. Bars, 5 µm. (m-n′′) Overexpression of *Notch^{NEXT}* in wild-type (m–m′′) or *dEHBP1^{O4}* (n–n′′) results in the development of extra Su(H)-positive socket cells. Single channel representations are shown for GFP (m–m′′) and Su(H) (n–n′′). Bars, 10 µm. (o–o′′) Overexpression of the variant *Delta $^{R+}$* in the absence of *dEHBP1* results in the development of extra Elav/HRP-positive neuronal cells, indicated by arrows. Overexpression of the variant *Delta $^{R+}$* is driven by the ubiquitous driver *tub^{Gal4}*, and therefore, we detect Delta in epithelial cells as well (left arrowhead). Single channel representations are shown for GFP (o′), Delta^{R+} (o′′), and Elav/HRP (o′′′). Bars, 10 µm.

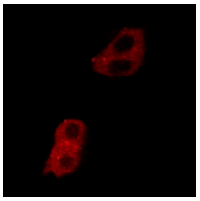

Video 1. **mCherry-dEHBP1 is localized within intracellular vesicles and at the interface of pIIa and pIIb cells.** Dividing cells in ESO clusters expressing mCherry-dEHBP1 by neur^{Gal4} driver were imaged by time-lapse confocal microscopy using an inverted laser scanning confocal microscope (model TE2000U; Nikon) equipped with a C1 confocal imaging system (488-, 543-, and 633-nm lasers; Nikon). Frames were taken every minute. Images are shown at the medial level of the cluster (related to Fig. 4).

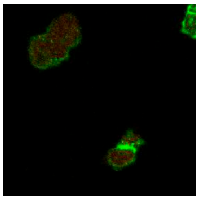

Video 2. **mCherry-dEHBP1 is localized partially with Spdo-GFP at the apical side of the interface of pIIa and pIIb cells.** Dividing cells in ESO clusters expressing Spdo-GFP and mCherry-dEHBP1 by neur^{Gal4} driver were imaged by time-lapse confocal microscopy using an inverted laser scanning confocal microscope (model TE2000U; Nikon) equipped with a C1 confocal imaging system (488-, 543-, and 633-nm lasers; Nikon). Frames were taken every minute. Images are shown at the apical level of the cluster (related to Fig. 4).

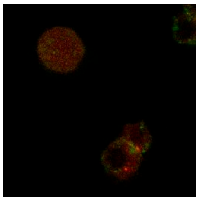

Video 3. **mCherry-dEHBP1 is localized partially with Spdo-GFP at the medial side of the interface of pIIa and pIIb cells.** Dividing cells in ESO clusters expressing Spdo-GFP and mCherry-dEHBP1 by neur^{Gal4} driver were imaged by time lapse confocal microscopy using an inverted laser scanning confocal microscope (model TE2000U; Nikon) equipped with a C1 confocal imaging system (488-, 543-, and 633-nm lasers; Nikon). Frames were taken every minute. Images are shown at the medial level of the cluster (related to Fig. 4).